学 位 論 文

Studies on the activation mechanism of Hedgehog signaling in fish

（魚類におけるヘッジホッグシグナル伝達経路の活性化機構の解析）

平成２５年７月博士（理学）申請

東京大学大学院理学系研究科

生物科学専攻

山 元　　孝 佳

Contents

Abbreviations

- *dhc2* *cytoplasmic dynein heavy chain 2*
- *dhh* *desert hedgehog*
- dpf days post-fertilization
- ENU N-ethyl-N-nitrosourea
- *fu* *fused*
- GFP green fluorescent protein
- HC heavy chain
- Hh hedgehog
- IC intermediate chain
- IFT intraflagellar transport
- *ihh* *indian hedgehog*
- KV Kupffer's vesicle
- LNT lateral neural tube
- M*dhc2* maternal mutant of *dhc2*

- MeOH methanol
- MO morpholino antisense oligonucleotide
- MZ*dhc2* maternal-zygotic mutant of *dhc2*
- ORF open reading frame
- PFA paraformaldehyde
- Ptch1 Patched 1
- *shh* *sonic hedgehog*
- Smo Smoothened
- VM ventral midline
- WT wild type
- *Zdhc2* zygotic mutant of *dhc2*

Abstract

Primary cilia are essential for Hedgehog (Hh) signal transduction in vertebrates. Although the core components of the Hh pathway are highly conserved, the dependency on cilia in Hh signaling is considered to be lower in fish than in mice, suggesting the presence of species-specific mechanisms for Hh signal transduction.

To precisely understand the role of cilia in Hh signaling in fish and explore the evolution of Hh signaling, I have generated a maternal-zygotic medaka (*Oryzias latipes*) mutant that lacks *cytoplasmic dynein heavy chain 2* (*dhc2*; MZ*dhc2*), a component required for retrograde intraflagellar transport. I found that MZ*dhc2* exhibited the shortened cilia and partial defects in Hh signaling, although the Hh defects were milder than zebrafish mutants which completely lack cilia. This result suggests that Hh activity in fish depends on the length of cilium. However, the activity of Hh signaling in MZ*dhc2* appeared to be higher than that in mouse *dhc2* mutants (also called *Dnchc2*), suggesting a lower requirement for cilia in Hh signaling in fish. I have revealed that the receptor Ptch1 is exclusively localized on the cilium in fish as in mammals. Subsequent

analyses revealed that Fused, an essential mediator for Hh signaling in *Drosophila* and fish but not in mammals, augments the activity of Hh signaling in fish as a transcriptional target of Hh signaling. The finding of this fish-specific augmentation provides a novel insight into the evolution of Hh signaling.

Introduction

Sexually reproducing multicellular organisms are developed from a single cell, a fertilized egg. Through numerous times of cell divisions, the egg gives rise to hundreds of different cell types, such as neurons, eyes, germ cells and muscles. These different tissues and organs do not exhibit random distribution but are organized with a remarkable reproducibility during development; eyes are always located on the head, not on our legs or arms, while the brain is placed inside the skull. How are these tissues and organs reproducibly orchestrated?

Morphogen gradient formation is a key concept for understanding these organizations. Morphogen is a diffusible molecule secreted into the extracellular space from its source and makes a concentration gradient. Multiple cell types are differentiated depending on its concentration, as in a model, so called "French flag model" (Rogers and Schier, 2011) (Fig. 1).

This concept of morphogen gradient has been used for understanding the regeneration of hydra and planarian flatworms since the 1700s. When these animals are

cut into two halves, the head half regenerates a tail, while the tail half regenerates a head half. This suggests that a kind of "polarity" is present along the body axis. In 1924, Spemann and Mangold discovered that transplantation of Spemann organizer, a cluster of dorsal cells in an amphibian gastrula embryo into the ventral region of a host gastrula induces a secondary axis, suggesting that inducing signals are released from the explant (Spemann and Mangold, 2001). In 1952, Turing proposed that chemical substances, called morphogens, can provide positional information for cells by making a concentration gradient (Turing, 1952).

Hedgehog (Hh) is one of the important morphogens in animal development, which is evolutionarily conserved from fly to human. Hh protein functions by binding to cell-surface receptor Patched, which serves as an inhibitor of Smoothened (Smo), a downstream membrane-bound mediator of Hh signaling. When Hh ligand binds to the receptor, the shape of Patched protein is altered so that it no longer inhibits the activity of Smo, thereby leading to the activation of Gli/Ci (short for Cubitus interruptus), a zinc finger containing transcriptional factor (Fig. 2).

hh was first identified as a segment polarity gene in *Drosophila* (Nusslein-Volhard and Wieschaus, 1980). Vertebrates have three homologues of the gene: *sonic hedgehog* (*shh*), *desert hedgehog* (*dhh*) and *indian hedgehog* (*ihh*) (Pathi et al., 2001). The expression patterns of these three paralogues are largely not overlapped. *dhh* is expressed in the Sertoli cells of the testes, essential for spermatogenesis and *ihh* is in the gut and cartilage. *shh* is expressed in many tissues, has the most variety of functions among the three homologues, and is essential for various aspects of embryogenesis including patterning events of the neural tube and limb (Huangfu and Anderson, 2006; McMahon et al., 2003). For example, in the neural tube, the sonic hedgehog (Shh) ligand forms a dorso-ventral (DV) gradient with the highest concentration ventrally, and specifies cell fates in a concentration-dependent manner (Dessaud et al., 2008). Thus, the expression of cell-type specific genes serves as a readout of Hh activity and delineates domains in the ventral neural tube (Fig. 3). The mechanism of Hh-signal transduction has been the target of intense studies but remains only partially understood.

One of the striking features of Hh signaling is that the primary cilium, a microtubule-based, immotile cellular protrusion, is essential in vertebrates but not in *Drosophila* (Wilson and Chuang, 2010). A requirement for the cilium in this pathway was first identified by genetic screening in mice for ciliary mutants exhibiting phenotypes similar to those of Hh-pathway mutants (Huangfu et al., 2003). However, subsequent genetic and molecular analyses demonstrated that cilium-dependency and the mediators of Hh signaling varies between fish and mammals, raising a question about conservation and evolution of the mechanism of Hh-signal transduction (Huang and Schier, 2009).

The formation and maintenance of cilia depend on the conserved process of intraflagellar transport (IFT) (Goetz and Anderson, 2010). Ciliary proteins are transported along the ciliary axoneme by IFT machinery, driven by kinesin-based anterograde and dynein-powered retrograde transport (Fig. 4).

In general, cilia are classified into two types; one is a motile cilium and the other is an immotile one, so called primary cilium. Motile cilia are present in some specific tissues such as the epithelium of the ventricle, trachea and oviduct. Defective

cilia have been implicated in numerous diseases termed ciliopathies, including hydrocephalus, bronchitis, infertility and *situs inversus*. Primary cilia are ubiquitously found on vertebrates cells with a few exceptions of myeloid and lymphoid (Wheatley, 1995). These cilia were first described in 1898 (Zimmermann, 1898), but their functions during animal development and physiology are only beginning to be unveiled (Eggenschwiler and Anderson, 2007).

Recently, the cilium was reported to resemble the nucleus in terms of the protein localizations and transport machinery. The nuclear import machinery including GTP-bound Ran and importin-β2 are also involved in ciliary import (Dishinger et al., 2010) and some nuclear pore complex proteins are located at the base of cilia and possibly function as a diffusion barrier (Kee et al., 2012). These results imply that cilia could have some essential roles in a transcriptional regulation.

Importantly, mammalian primary cilia have been recently shown to mediate transduction of Hedgehog (Hh) signals (Huangfu et al., 2003; Wilson and Chuang, 2010). Further analysis provided that several key components of Hh pathway are enriched in cilia, including Ptch1, Smo and Gli transcription factors (Goetz and

Anderson, 2010). In the absence of Ift88, a component of anterograde IFT machinery, both mouse and zebrafish embryos lack cilia and exhibit a severe reduction in Hh signaling. However, the phenotype is milder in zebrafish. In the neural tube, most of the Hh target genes are not expressed in mouse mutants, while the expression of low-threshold genes remains and expands in zebrafish (Huang and Schier, 2009; Huangfu et al., 2003). These results suggest that cilium is required for Hh signaling also in fish, but the dependency on cilia is lower than that in mammals. However, it was still unclear how much Hh signaling in fish depends on cilia and what is the underlying mechanism for that difference.

Furthermore, Fused (Fu), a putative serine-threonine kinase, first identified as an essential mediator of Hh signaling in *Drosophila*, turned out to be not required for mammals, but it is indispensable for zebrafish (Chen et al., 2005; Merchant et al., 2005; Wilson et al., 2009; Wolff et al., 2003). These facts suggest that the pathway in zebrafish is more similar to that in *Drosophila* or placed in between *Drosophila* and mammals, making fish a unique model with which to investigate the transition state from an ancestral to a modern type of Hh signaling.

To further address the difference and the evolution of Hh signaling among species, I have generated a maternal-zygotic (MZ) medaka mutant that lacks *cytoplasmic dynein heavy chain 2* (*dhc2*), an essential component of retrograde IFT, and compared the neural phenotypes of medaka and mouse *dhc2* mutants (also called *Dnchc2*, especially in mouse). I have generalized that the requirement for cilia in Hh signaling is lower in fish than in mammals. Additionally, the receptor Ptch1 is localized to cilia in fish as in mammals. Subsequent analyses revealed that the difference in the requirement for cilia in Hh signaling across vertebrates can be interpreted by differential regulation and function of Fu.

Results

Generation of maternal-zygotic *aA90*/*dhc2* mutants

The medaka *aA90* (*Zdhc2*) mutant, isolated in an ENU-induced mutagenesis screening (Yokoi et al., 2007), is a recessive lethal mutant showing defects in left-right (L/R) axis determination (Fig. 5A-B; Table 1). L/R asymmetry is established by directional flow of extra-embryonic fluid surrounding the node (Kupffer's vesicle in fish) by cilia (Nonaka et al., 1998). To identify the defective gene in the *aA90* mutant, Dr. Tadashi Ishiguro (a previous undergraduate student) carried out positional cloning and narrowed down the *aA90* locus to a 250 kb region in linkage group 13, which harbors one open reading frame, *cytoplasmic dynein heavy chain 2* (*dhc2*), an IFT retrograde component (Fig. 4, 6A). He found that *aA90* has a 37.7 kb deletion in the *dhc2* locus including the start codon, the heavy chain (HC)-HC and the HC-Intermediate chain interaction domain, and the AAA ATPase domain (Fig. 6A, C). Database searches demonstrated that the *dhc2* gene exists as a single copy within the medaka genome. I injected antisense morpholinos (MO) against the *dhc2* gene into wild-type embryos significantly

phenocopied *aA90*, which led me to conclude that *dhc2* is the gene deficient in the *aA90* mutant (Table 1). I named *aA90* mutant as *dhc2* mutant in the following description.

Probably due to the maternal contribution of *dhc2*-gene products, the phenotype of *dhc2* mutants was mild. For example, only one-fourth of the *dhc2* homozygous mutants showed *situs inversus* (Table 1). To completely eliminate *dhc2* products, I have generated maternal-zygotic *dhc2* (MZ*dhc2*) mutants using the germline-replacement technique (Ciruna et al., 2002; Shimada and Takeda, 2008) with the following modifications (Fig. 7). For making a maternal-zygotic medaka mutant, it is known to use the interspecific hybrid sterility of Japanese (Kaga) and Chinese (Hainan) medaka as hosts for transplantation of germ cells from homozygous donors followed by sterility check of the hosts after sexual maturation (Shimada and Takeda, 2008). The hybrid, however, does not produce many eggs. In zebrafish, the knockdown technique using morpholino against an essential gene, *dead end*, for the primordial germ cell (PGC) has been used for making a maternal zygotic mutant (Ciruna et al., 2002). I decided to apply the zebrafish knockdown method to medaka. As a host, I used *olvas*-GFP transgenic medaka, whose oocytes were labeled with green fluorescent

proteins using the regulatory region of the medaka *vasa* gene (*olvas*, named after *Oryzias latipes vasa*) (Tanaka et al., 2001), so that I easily check whether they have germ cells or not. To label donor cells, I injected the rhodamine-dextran (10 kDa; Molecular Probes, D1816), instead of "fixable" rhodamine dextran (10 kDa; Molecular Probes, D1817) which was frequently used in medaka transplantation experiments, considering the toxicity for the early embryogenesis in medaka. Host embryos were injected at one-cell stage with 300 μM of a morpholino antisense oligonucleotide directed against *dead end* mRNA and checked the loss of their germ cells at 2 dpf by the loss of GFP fluorescence. Donor embryos were genotyped to identify homozygous embryos. The other procedures were done according to the previous report (Shimada and Takeda, 2008). Crosses of females with mutant germ cells and heterozygous males (*dhc2*/+) generated 50% homozygous mutants that lacked both maternal and zygotic products of *dhc2* (M*Zdhc2*) and 50% heterozygous mutant embryos that lacked only the maternal *dhc2* contribution (M*dhc2*). As expected, hosts produced many eggs like wild type adults.

The complete loss of *dhc2* activity increased the frequency of *situs inversus* to 52.8% (Table 1, Fig. 5A-D) as well as enlarged ventricles and expanded nephric duct (Fig. 5E-H, M-P). Moreover, the typical phenotypes of defective Hh-signaling, severe ventral curvature and U-shaped somites instead of chevron-shaped ones, were observed in M*Zdhc2* mutants, but not in zygotic (*Zdhc2*) or M*dhc2* mutants (Fig. 5I-L, Q-T), indicating reduced levels of Hh signaling. Importantly, the morphology of cilia was dramatically shortened in M*Zdhc2* as demonstrated by scanning electron microscopy (SEM) (Fig. 8A). To expose the ventricular surface area of neural tubes, I exteriorized this area with forceps, prior to fixation (Fig. 8B) and found that cilia on the surface of non-floor plate (FP) neuroepithelial cells (LNT, lateral neural tube) and longer ones on the FP cells (VM, ventral midline) were much shorter and bloated in M*Zdhc2* than their wild-type counter parts (Fig. 8A). In the Kupffer's vesicle and somites, cilia were also shortened in M*Zdhc2*, as compared with those in WT, M*dhc2* and *Zdhc2* (Fig. 8C, data not shown). The number and morphology of cilia in *Zdhc2* mutants appeared normal at least until the segmentation stages, but subtle defects in function or lately overt defects could account for their milder phenotypes (Table 1, data not shown). The ciliary

phenotypes in MZ*dhc2* mutants are nearly identical to those in mouse *dhc2*/*Dnchc2* mutant (Huangfu and Anderson, 2005; May et al., 2005), and thus the analysis of the Hh activity in MZ*dhc2* mutants enabled us to examine differences and distinct mechanisms between fish and mouse in the requirement for cilia in Hh signaling.

Patterning of the spinal cord in MZ*dhc2* mutants

As described in Introduction (Fig. 3), depending on the Hh gradient, the vertebrate neural tube exhibits position-specific gene expression along the dorso-ventral axis; roughly from ventral to dorsal, *foxa2* in the FP, *nkx2.2* in p3 neuron precursors, *olig2* in motor neuron precursors (pMN), *nkx6.1*/*6.2* in p3/pMN/p2 progenitors, and *pax6, pax3*, *dbx1* and *dbx2* in dorsally located neuron precursors and their expressions are mutually exclusive underlined by their repressive interactions (Fig. 3) (Dessaud et al., 2010; Jeong and McMahon, 2005). Shh is known to induce the expression of the ventral genes (*foxa2*, *nkx2.2*, *olig2*, *nkx6.1*and *nkx6.2*), while suppressing the dorsal genes (*pax6, pax3*, *dbx1* and *dbx2*) (Balaskas et al., 2012; Dessaud et al., 2010; Jeong and McMahon, 2005). I first confirmed that *shh* was normally expressed in the medial FP (MFP) and

underlying notochord of MZ*dhc2* mutants (Fig. 9A, 10J), suggesting that defects observed in mutants are mainly ascribed to signal transduction defects.

In MZ*dhc2* mutants, *foxa2* and *nkx2.2* were expressed (Fig. 9A, 10H-I), and ventral intermediate genes, *olig2*, *nkx6.1* and *nkx6.2* were dorsally expanded, whereas this dorsal expansion was not observed in Z*dhc2* (Fig. 9A, 10E-G).

The expression of these ventral genes suggests that the Hh pathway is activated in cells with severely shortened cilia and even reaches the high levels of activation, not missing the expression of the most ventral side genes. Additionally, like zebrafish, the most ventral gene *foxa2* expression in the medial FP is Hh-independent in medaka embryos (Fig. 11B), and thus I will use *nkx2.2* expression as a marker of the high level of Hh activation. Also, it is worth noting that the most ventral region appeared to be missing in MZ*dhc2* embryos, because the expression domains of *nkx2.2*, which are normally separated by the negative medial FP cells, frequently merged in the medial region (Fig. 9A). However, due to the lack of a specific marker for this region, I was unable to determine the cell type specifically defective in MZ*dhc2* embryos.

The expansion of lower-threshold gene expression (*olig2*, *nkx6.1* and *nkx6.2*) also suggests that the area of low Hh activation abnormally expanded dorsally in the mutant neural tube, probably because shortened cilia in MZ*dhc2* could not retain Hh ligand, leading to dorsally expanded distribution of the ligand (further analysis and discussion are described in the result of "MZ*dhc2* cells are less sensitive to Shh" and discussion section). Dorsal expansion of *olig2* expression in MZ*dhc2* was also observed at three different anterior-posterior axis levels (Fig. 12). This was further supported by dorsally retracted expression of *pax6*, *pax3*, *dbx1* and *dbx2*, observed in MZ*dhc2* mutants (Fig. 9A, 10A-D), reflecting the repressive interactions of these genes.

In *Dnchc2*-mutant mice, *nkx2.2* expression was reported to be lost, but *olig2* was expanded (Huangfu and Anderson, 2005; May et al., 2005). Thus, there are similarities and differences in the neural tube phenotypes between fish and mouse *dhc2* mutants (Fig. 13), both of which I addressed in the following experiments.

Lower Hh pathway activation in mutant cells

To examine the activation level of Hh pathway in mutant cells, I treated MZ*dhc2* embryos with various concentrations of cyclopamine, a potent antagonist of Smoothened (Smo). Intriguingly, in the MZ*dhc2* group, the percentage of *nkx2.2*-positive embryos started to decrease at a cyclopamine concentration as low as 0.25 μM, and went down below 50% at 0.5 to 1 μM, while at such low concentrations, 100% of embryos maintained *nkx2.2* expression in the wild-type and M*dhc2* groups (Fig. 14A, C; Table 4). These results suggest that the activity of Hh signaling in mutant cells is compromised at the level or upstream of Smo, but still high enough to express the ventral-most marker, *nkx2.2*.

Zebrafish mutants with complete lack of cilia were reported to be insensitive to cyclopamine and dominant-negative (dn) PKA (Ben et al., 2011; Huang and Schier, 2009), which induces ectopic Hh-pathway activation downstream of Smo. By contrast, MZ*dhc2* is sensitive to cyclopamine (Fig. 14A, C) and dnPKA (Fig. 15), probably because they have shortened but certain cilia. This discrepancy can be explained by the fact that cilia are required for both Smo and PKA activity in fish. This is why the

M*Zdhc2* mutant is sensitive, and the mutants with a complete loss of cilia are not sensitive, to cyclopamine and dnPKA.

Patched1 localizes to cilia in medaka fish

In murine cells, Hh receptor Patched1 (Ptch1) was reported to localize the primary cilium at least in cultured cells and paraxial mesoderm cells (Ocbina et al., 2011; Rohatgi et al., 2007), whereas it is not the case in *Drosophila*, which does not require cilia for the reception of Hh (Wilson and Chuang, 2010). However, the receptor localization was unknown in fish. Two homologues (*patched1* and *patched2*) of *Drosophila patched* were isolated in fish. To distinguish these two paralogues, I made the phylogenic tree of these *patched* genes (Fig. 16A). As a result, medaka Ptch1 is the homologue of mammalian Ptch1, which is a receptor of Shh. For further confirmation, I knocked down Ptch1 in medaka and analyzed the Hh activity. In the morphants, the number of Engrailed (a Hh target gene) expressing cells in somites was increased (Fig. 16B), representing the increased Hh activation due to the lack of the receptor, similar to zebrafish morphant (Wolff et al., 2003). These results indicate that Ptch1 is the receptor

of Hh in medaka. To analyze the receptor localization in medaka, I generated an antibody against the extracellular domain of medaka Ptch1 (Fig. 16C), and examined the distribution of Ptch1 in wild-type and MZ*dhc2* neural-tube cells. Firstly, the specificity of the antibody was confirmed by knockdown and overexpression experiments (Fig. 16D, E). As shown in Figure 16D, in WT, Ptch1 was localized to the cilia of neuroepithelial cells which were exteriorized with forceps before fixing (Fig. 8B). Importantly, Ptch1 was still localized to severely shortened cilia in MZ*dhc2* (Fig. 16D). These results indicate that the cilium is the site for Hh receptor Ptch1 localization in medaka.

MZ*dhc2* cells are less sensitive to Shh

Although the activation level of Hh signaling is still sufficient to induce all target genes in MZ*dhc2* cells, the amount of Ptch1 in severely shortened cilia is likely to be decreased. This could explain the higher sensitivity to cyclopamine in MZ*dhc2* than that in WT in the above experiment (Fig. 14A, C). In other words, MZ*dhc2* cells could be less sensitive to Shh. Although the transplantation of mutant cells into wild-type neural

tubes was a straight way to test this idea, I thought that it was hard for me to detect the loss of target gene expression in a single cell embedded in cells positive for target gene expression. Thus, I transplanted wild-type cells into MZ*dhc2* blastula or M*dhc2* (control), and examined *olig2* expression when donor cells were localized in host neural tubes (Fig. 17A). I distinguished MZ*dhc2* from M*dhc2* embryos by the eye phenotype at 16-somite stage when transplanted embryos were fixed for the analysis (Fig. 17B). The defect in eye formation can be explained by the fact that the rods and cones of the retina consist of highly modified cilia. Remarkably, *olig2*-positive WT cells were frequently found in the region more dorsal to the host *olig2*-expression domain in MZ*dhc2* embryos (Fig. 17C, WT to MZ*dhc2* (right panel), arrowhead; n=9/10), while no such ectopic expression was detected in control transplants (Fig. 17C, WT to M*dhc2* (left panel), arrowhead; n=15/15). These results demonstrate that Hh-activation of MZ*dhc2* cells is lower than that in WT cells, even if they are exposed to the same concentration of Hh-ligand. Additionally the ectopic expression suggests that the distribution of Hh ligand is dorsally expanded in MZ*dhc2*, due to the decreased number of the receptor available on the cell surface.

Fused forms a positive-feedback loop in fish

The presence of *nkx2.2* expression is unique in MZ*dhc2*, considering that mouse *Dnchc2* mutants lose *nkx2.2* expression (Huangfu and Anderson, 2005; May et al., 2005). The same tendency was observed in the expression analysis of Hh target genes of *ift88* mutants in zebrafish and mouse that completely lack cilia; only zebrafish mutants maintain the expression of intermediate genes like *olig2* (Huang and Schier, 2009; Huangfu et al., 2003), implying that the activation of Hh signal is enhanced in fish. To explore a teleost-specific mechanism, I focused on *fused* (*fu*), an intracellular mediator of Hh signaling downstream of Smo in *Drosophila*, which has evolved divergent roles in the vertebrate lineage: one for Hh signaling and the other for ciliary motility. Interestingly, murine *Fu* is not involved in Hh signaling and specifically participates in the motility of cilia, whereas it is required for both in zebrafish (Wilson et al., 2009; Wolff et al., 2003). I first tested whether *fu* is essential for Hh signaling in medaka by injecting *fu* MO (600 μM) targeted to the splicing site (Fig. 18A) and observed the loss of *nkx2.2* expression (Fig. 18B; n=14/15). Additionally, morphants injected together

with *fu* mRNA rescued *nkx2.2* expression (Fig. 18C; n=14/14) and injection of *fu* mRNA into WT embryos elevated Hh activity as indicated by the expansion of the ventral intermediate genes, *olig2* and *nkx6.1* (Fig. 18D; n=9/14, 9/9, respectively). I then knocked down *fu* in MZ*dhc2* mutants to see if the remaining expression of Hh target genes in those mutants also depends on Fu. However, under this experimental conditions, most of the MZ*dhc2* mutants injected with *fu* MO (600 μM) died probably due to a requirement of Fu in earlier development (Xia et al., 2010), and I therefore reduced the concentration of *fu* MO (300 μM), when injected into MZ*dhc2* mutants. These injected MZ*dhc2* embryos failed to express *nkx2.2* (Fig. 18B). Interestingly, the expansion of the ventral intermediate gene, *olig2*, was also rescued (Fig. 18B). These results demonstrate that *fu* is indispensable for Hh signaling in wild-type and mutant medaka embryos and its overexpression augments the signal.

fu is known to be expressed ubiquitously in zebrafish at early developmental stages (Xia et al., 2010), but the precise pattern and regulation of *fu* expression during neural tube patterning have not been reported. My further analysis revealed that *fu* expression is restricted to the ventral part of neural tube where high to low levels of Hh

signaling are activated at 16-somite stage in medaka (Fig. 19A). Furthermore, *fu* expression was dorsally expanded in MZ*dhc2* neural tubes (Fig. 19A), like the ventral intermediate genes. These results suggest that *fu* is a transcriptional target of Hh signaling. To test this possibility, I treated wild-type embryos with 5 μM cyclopamine and observed severe reduction or loss of *fu* expression in cyclopamine-treated embryos (Fig. 19B), indicating that *fu* expression is induced by Hh signaling downstream of Smo. I also confirmed that *fu* expression in zebrafish is ventrally restricted in the neural tube and depends on Hh signaling (Fig. 19C).

I finally asked if Fu, when overexpressed, can restore Hh signaling, when Smo-mediated signaling is compromised. For this, embryos were treated with 2.5 μM cyclopamine (intermediate dose, Fig. 14A) together with *fu* mRNA injection. Those injected embryos showed weak but significant up-regulation of *nkx2.2* (n=12/18) as compared with cyclopamine-treated control embryos (n=1/14) (Fig. 19D), suggesting that Fu augments Hh activity downstream of Smo. Given that Fu is a positive mediator of Hh signal transduction, Fu is likely to form a positive feedback loop downstream of Smo to reinforce Hh signal in teleost target cells (Fig. 20).

Discussion

In the present study, utilizing the medaka mutant with severely shortened cilia, MZ*dhc2*, I demonstrated that shorter cilia mediate less Hh activation in fish, although the Hh defects were milder than zebrafish mutants which completely lack cilia. This result suggests that Hh activity in fish depends on the length of cilium. And I also found that the receptor Ptch1 is localized on the cilium in fish. These are largely consistent with the observation of murine ciliary mutants. Furthermore, the present study has addressed why the expression of low-threshold target genes is expanded in ciliary mutant neural tubes and how Hh signal is augmented in fish mutant cells.

A possible role of cilia in Hh gradient formation

olig2-positive wild-type cells in MZ*dhc2* neural tubes were positioned more dorsally than dorsal boundary of *olig2* expression in wild-type neural tubes (Fig. 17C). This result, though indirectly, suggest that the gradient profile of Hh ligand dorsally shifts in the mutant neural tubes. Additionally, consistent with this result, when I treated the

mutant embryos with various concentrations of cyclopamine, in the WT and M*dhc2* group, the percentage of *olig2*-positive embryos started to decrease at a cyclopamine concentration as low as 2.5 μM, and went down below 27% at 5 μM, while 78% of embryos maintained *olig2* expression in the MZ*dhc2* groups (Fig. 14B). These results indicate that in the case of the lower threshold *olig2* expression, the activity of Hh signaling in mutant cells is enhanced, probably because the gradient of Hh ligand was dorsally expanded in the mutant embryos.

Dorsal expansion of Shh ligand was directly observed with *smoothened* mouse mutants (Chamberlain et al., 2008) and this can be interpreted as a consequence of the reduced amount of Ptch1 receptor, a downstream target of Hh signaling. Indeed, it has been proposed that the Shh gradient is regulated by a Shh-induced negative-feedback mechanism in which ligand binding to Ptch1 at the cilia sequesters Hh ligand itself in the intercellular space (Jeong and McMahon, 2005). It is thus conceivable that in ciliary mutant neural tubes, the reduced amount of Ptch1 on cilia caused a dorsally shifted Hh gradient (Fig. 17C), and thereby the expression domain of ventral low-threshold target genes is expanded, although further confirmation by direct imaging is required.

Consistently, the neural tube in *Dnchc2* mutants also exhibits the expansion of low threshold gene expression (Huangfu and Anderson, 2005; May et al., 2005). Thus in vertebrates, the length of cilia (or the receptor Ptch1) could be one of the factors that affect the Hh gradient in the neural tube.

Importance of cilia in Hedgehog signaling

In the present study, I generalized that cilium is required for Hh signaling in fish. Additionally, the receptor Ptch1 was found to localize the cilium, as in mouse.

Considering the advantages of the use of cilia in Hh signal transduction, the efficiency for signal transduction could be increased if cilia are centered. The length of primary cilium is around 1-10 μm and the width is 500 nm. The volume of the cilia is around 1/10000 of cytosol. They can thus concentrate signal-transducing molecules 10000 times higher if the molecules are only localized to the cilia; in the case of 1 μM molecules localized to cilia, around 600 molecules are in the cilia, suggesting that the efficiency for signal transduction could be greatly increased. Additionally, as described in Introduction, cilia are thought to resemble the nucleus because of the high

concentration of GTP-bound Ran in the cilia and some nuclear pore proteins localized at the ciliary base (Dishinger et al., 2010; Kee et al., 2012). Cells could use cilia to form a compartment which is distinguished from the cytoplasm. In the case of Hh signaling, the ciliary compartment is a good place to avoid mis-activation of the target genes through ciliary sequestration of its transcription factor Gli. Additionally, considering that a ciliary localization signal is known to be similar to a nuclear localization signal (Dishinger et al., 2010), the translocation of ciliary proteins to the nucleus could be a relatively easy strategy. Given that the use of the cilium has many advantages as described above, fishes have evolved to use the cilium as a center of Hh signaling. Furthermore, in addition to Ptch1, Smoothened in fish is known to localize to the cilium, as in mammals (Aanstad et al., 2009). On the other hand, fishes maintain the *fused*-mediated pathway which is lost in mammals. These facts highlight fish as a unique model with which to investigate the transition state from non-cilia to cilia-mediated Hh signaling.

Significance of teleost-specific augmentation of Hh signaling mediated by Fused

In the present study, I propose that Fu is a key component to account for the difference in activation level between mammals and fish in ciliary mutants. Fused is a crucial mediator of Hh signaling in *Drosophila* and zebrafish, but not in mammals (Wilson et al., 2009). I first confirmed that *fu* is required for Hh signaling in medaka like zebrafish, and next found that the expression of *fu* in the neural tube is restricted to the ventral part and induced by Hh signaling in fish. Subsequent analyses demonstrated that Fu forms a positive-feedback loop downstream of Smo (Fig. 20); Fu activates the Hh pathway which then leads to the up-regulation of Fu. The positive feedback centered by Fu could augment Hh signal in ciliary mutant cells with lower input of Smo-mediated signaling. This could thus explain why the phenotype of fish ciliary mutants is milder than that of mammalian counterparts. Of course, Fu may not be a mere component that differentiates the ciliary dependency in the two vertebrate models. Indeed, in zebrafish, low levels of Hh activation mediated by Gli1 is known to occur in an Hh-independent manner and its mechanism remains elusive (Huang and Schier, 2009).

What is the biological and evolutionarily significance of the positive-feedback mechanism in Hh signaling? A hint could be found in the speed and mode of neurulation in fish. According to the recent report by Xiong et al. (2013), specification of neural cell types in zebrafish begins earlier and proceeds faster under the noisy conditions of cell movements in the formation of the neural keel, whereas in other vertebrates, such as chick and mice, neurulation proceeds gradually and steadily in an epithelialized cell sheet, following an established Shh gradient. A rapid and amplified response to Shh in target cells would thus be necessary in fish neurulation.

Additionally, the size of neural tube in medaka is about one-fourth as large as that in the mouse. To make Hh gradient correctly in the ventricular zone in medaka, similar to that in mouse, it is likely that the amount of Hh ligands is lower in medaka, suggesting the requirement of augmentation of Hh signaling in fish. Of course, the quantification and/or the imaging of the ligand will be necessary to discuss this further.

Xiong et al. (2013) also showed that specified neural progenitors sort to form sharply bordered domains from mixed progenitor populations. However, this apparently contradicts the transplantation result showing ectopic expression of a specific marker in

wild-type donors (Fig. 17C), suggesting that multiple strategies, including sorting and position-dependent determination, are employed to achieve a robust patterning.

Finally, the presence of cilium-mediated signaling was recently reported in the olfactory epithelium of *Drosophila* (Kuzhandaivel et al., 2014), suggesting the evolutionarily ancient origin of this mechanism. Thus, further analysis of Hh signaling in diverse species and tissues will provide greater insight into the evolution of this crucial signaling pathway.

Conclusions

The present study not only strengthens the idea of a conserved role of primary cilia in Hh-signal transduction in vertebrates, but also uncovered a teleost-specific augmentation mechanism mediated by Fu. The fish-specific augmentation can serve as the mechanism that accounts for the lower cilia-dependency for Hh signaling in fish and gives novel insight into the evolution of Hh signaling.

Materials and methods

Fish strains

All studies of medaka (*Oryzias latipes*) were carried out using d-rR strain of a closed colony. ENU-based mutagenesis of medaka was performed as described previously (Ishikawa, 1996). Zebrafish (*Danio rerio*) were Riken wild-type, strain RW. Fish stocks were maintained under a long-day photoperiod of 13.5:10.5 h light:dark at 28 °C. Under these conditions, medaka spawn daily within 1 hour of the onset of light for a number of consecutive days, zebrafish spawn about once per two weeks. Collected medaka embryos were sorted into medaka Hatching buffer, maintained at 32°C, and staged according to morphological criteria (Iwamatsu, 2004). For zebrafish, the embryos were sorted into 1/3 Ringer (39 mM NaCl, 0.97 mM KCl, 1.8 mM $CaCl_2$, 1.7 mM HEPES at pH 7.2) and maintained at 28.5°C and staged according to hours postfertilization (hpf) at 28.5°C and morphological criteria (Kimmel et al., 1995). All experimental procedures and animal care were carried out according to the animal ethics committee of the University of Tokyo.

Genotyping of medaka *aA90/dhc2* mutant

A small segment of caudal fin was excised and fix them in 100% MeOH. And genomic DNA was extracted with 50 µl of DNA extraction buffer [10 mM Tris pH 8.0, 50 mM KCl, 0.3% Tween20, 0.3% NP40 and 1 mg/ml proteinase K (Invitrogen)] at 55°C overnight. The sample was then heated to 98°C for 10 min to inactivate proteinase K and centrifuge at 15.3 kG, 4°C, 10 min and 2 µl of the supernatant of each sample was used as a template for polymerase chain reaction, PCR (total volume 10 µl). PCR primers were described in Table 2.

Antibody generation

His-tagged N-terminal (169-405; Ptch1-N-His) polypeptide of medaka Ptch1 (Fig. 16C) was expressed in *E. coli* Rosetta (DE3) competent cells using pET24a (Novagen) vector. Recombinant proteins were purified with Profinity™ IMAC Ni-charged resin (Bio-Rad) under denaturing conditions and dialyzed against PBS. This Ptch1-N-His polypeptide was used for immunization of rabbits. Anti-medaka Ptch1-N-His (169-405) antibody

was affinity-purified using Immobilon membrane (Millipore) strips onto which the antigen were transferred as described (Okano-Uchida et al., 2003).

Whole mount *in situ* hybridization

Embryos were fixed with 4% paraformaldehyde (PFA) in PBST (phosphate-buffered saline containing 0.1% Tween-20) overnight and dechorionated manually with forceps, then stored in MeOH at –20°C. After rehydration, embryos were permeabilized with proteinase K (10 μg/ml) at room temperature for 7 minutes and re-fixed with 4% PFA/PBST for 25 min. The specimens are washed five times in PBST. Hybridization was carried out at 65°C with digoxigenin-labeled probes overnight. Hybridized embryos were washed with 50% formamide/2xsaline-sodium citrate (SSC)-0.1% Tween20 (SSCT), 2xSSCT and 0.2xSSCT, incubated in 0.2% blocking reagent (Roche) at room temperature for more than 2 hours, and then treated with anti-digoxigenin antibodies labeled with alkaline phosphatase (Roche) at 1:7000 dilution with 0.2% blocking reagent. The staining reaction was started by incubating medaka embryos with NBT/BCIP solution according to the protocol described for the NBT/BCIP ready-to-use

tablets (Roche), zebrafish embryos with BM Purple (Roche). The cDNAs used as the templates for the probes were described in Table 2.

mRNA overexpression

mRNAs were synthesized as reported previously (Yokoi et al., 2007). Briefly, to synthesize RNA *in vitro*, the open reading frame of the medaka *ptch1* and *fused* were cloned into the pCS2+ vector. The dominant-negative regulatory subunit (R1α) for murine PKA (dnPKA) was kindly provided by Dr. Anna Wild (Univ. of Sheffield). Capped sense RNA was synthesized using mMESSAGE mMACHINE® SP6 Transcription Kit (Ambion). The synthesized RNA was purified using the RNeasy Mini kit (QIAGEN) and stored at −80°C until use.

Microinjection and Cell transplantation

To generate the maternal-zygotic *aA90*/*dhc2* mutant, donor embryos were obtained from intercrosses of *aA90*/*dhc2* heterozygous fish; host embryos were from *olvas*-GFP transgenic fish, whose oocytes were labeled with green fluorescent proteins using the

regulatory region of the medaka *vasa* gene (*olvas*, named after *Oryzias latipes vasa*) (Tanaka et al., 2001). Donor embryos were injected at one-cell stage with 10 mg/ml rhodamine-dextran (10 kDa; Molecular Probes). Host embryos were injected at one-cell stage with 300 μM of a morpholino antisense oligonucleotide directed against *dead end* mRNA. At morula stage, donor and host embryos were dechorionated with hatching liquid (Yasumasu et al., 1989). At mid-blastula stage, the embryos were placed on V-shaped grooves of a 1.5% agarose gel immersed in Yamamoto's Ringer (Yamamoto, 1956), and then the 50–100 cells were transplanted from the margin of donor embryos into the animal pole of similarly staged hosts using a micromanipulator (M-152, Narishige) in combination with a microinjector (IM-6, Narishige). Transplantation needles were made from a glass capillary (G-1, Narishige) pulled by a horizontal pipette puller, and clipped with forceps to form a sharp tip. Donors and hosts were cultured individually in glass dishes until 2 dpf; host embryos were then screened for the transfer of fluorescently labeled donor-derived PGCs, and donor embryos were genotyped for *dhc2*. To confirm the PGC elimination in host germ cells, these host embryos were

checked whether GFP signals were disappeared at hatching stage. If germ cells elimination were not succeeded, the offsprings will have GFP fluorescent signals.

For normal cell transplantation, donor embryos were injected with the mixture of rhodamine- and biotin-dextran. At mid-blastula stage, scores of cells were transplanted into the margin of donor embryos to make mosaic neural tube.

Histology

The paraformaldehyde-fixed fish embedded with 1.5% Agarose in 1/2 hatching buffer were dehydrated in a graded series of ethanol-water mixtures, then incubated in 1:1 ethanol and infiltration solution (Technovit 7100, Heraeus Kulzer) for 30 min. The specimens were incubated in infiltration solution for at least 4 hours and positioned in polymerization medium (Technovit 7100, Heraeus Kulzer) overnight at 4°C and sectioned with RM2245 (Leica) at a 7-12 μm thickness. Microtome sections were prepared and mounted on slides, air dried at 30°C, stained with Nuclear fast red (Vector) or Mayer's Hematoxylin Solution, overlaid with rapid mounting medium (Entellan new, Merck), and cover-slipped.

Immunohistochemistry

For immunohistochemistry, medaka embryos were dechorionated using hatching liquid in 1/2 Yamamoto Ringer, fixed with 4% PFA/PBS for 1 hour at room temperature, permeabilized with 0.5% Triton X-100 in PBS at room temperature for 30 min, rinsed with PBS, incubated in blocking solution (2% BSA, 10% DMSO, and 0.2% Triton X-100 in PBS) for 1 hour at room temperature, and then incubated with primary antibodies in blocking solution overnight at 4°C: Ptch1 at 1:200; Monoclonal anti-acetylated α-tubulin antibody (T6793, Sigma) at 1:400; monoclonal anti-γ-tubulin antibody (T3559, Sigma) at 1:1000. After washing in PBSDT (1% DMSO and 0.1% Triton X-100 in PBS), embryos were incubated with Alexa 488, 555 or 647 (Molecular Probes) conjugated secondary antibodies at 1:400 in blocking solution overnight at 4°C. Embryos were washed with PBSDT at room temperature after incubation with each antibody. Washed embryos were cleared in 50% glycerol/PBS and photographed on a LSM710 confocal fluorescence microscope (Zeiss). For the cilia staining of neural tube,

the apical surface were exteriorized with forceps prior to fixation. Next steps are according to the normal immunohistochemistry protocol.

Chemical treatment

The chorion was manually removed using hatching liquid for medaka and 5 mg/ml pronase for zebrafish, prior to the incubation. To inhibit Hh signaling dechorionated embryos were incubated from 30-50% epiboly stage in cyclopamine (BML-GR334, Enzo Life Sciences). Control embryos were treated simultaneously with an equal concentration of DMSO.

RT-PCR

RT-PCR analysis was performed using total RNA of medaka embryos. Total RNA was isolated from medaka embryos at the late gastrula stage using ISOGEN (Nippon gene), according to the manufacturer's instructions. First-strand cDNA was prepared from 5 μg total RNA using an oligo d(T) primer and SuperscriptIII reverse transcriptase

(Invitrogen) and cDNA fragments were obtained by PCR with the primers described in Table 2.

PCR fragments were then cloned into the pCRII-TOPO vector (Invitrogen). For the RNA probe synthesis, the insert was transcribed *in vitro* with SP6 or T7 RNA polymerase (Promega) after linearization of the plasmid.

Scanning electron microscope

Medaka embryos were dechorionated using hatching liquid in 1/2×Yamamoto ringer. Apical surfaces of neural tube were exteriorized with the forceps. These embryos were immediately fixed in 2.5% glutaraldehyde (TAAB), 2% paraformaldehyde (Thermo) in 0.1 M sodium phosphate buffer pH 7.4 (Wako) for 18 hours at 4°C. These embryos were postfixed in a 1% osmium tetroxide solution (TAAB) for 2 hours at 4°C, dehydrated in an ascending series of ethanol and infiltrated with *t*-butyl alcohol (Nacalai). The specimens were frozen at 4°C, freeze-dried, mounted on aluminums tubs with double-sided adhesive tape, coated with platinum, and viewed at 10 kV on a Hitachi S-800 scanning electron microscope.

Figures

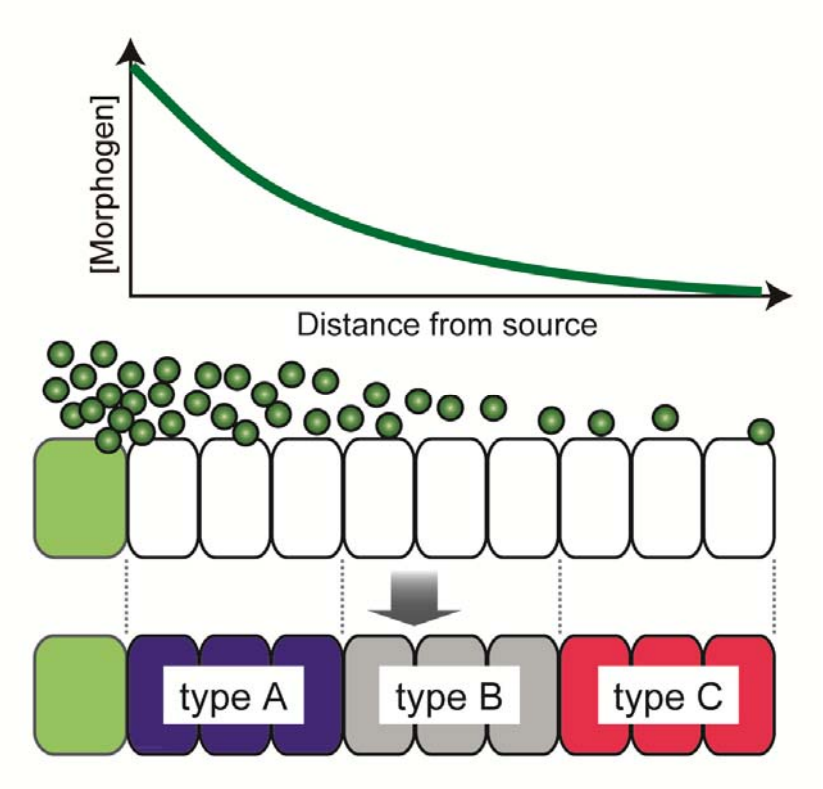

Figure 1. The French flag model providing a positional information by a morphogen concentration gradient.

In this model, the positional information is delivered by a gradient of a diffused morphogen extended from a source cell (green). Morphogen forms a concentration gradient at the extracellular space. Multiple cell types are differentiated in a concentration dependent manner. Figure based on Rogers & Schier, 2011.

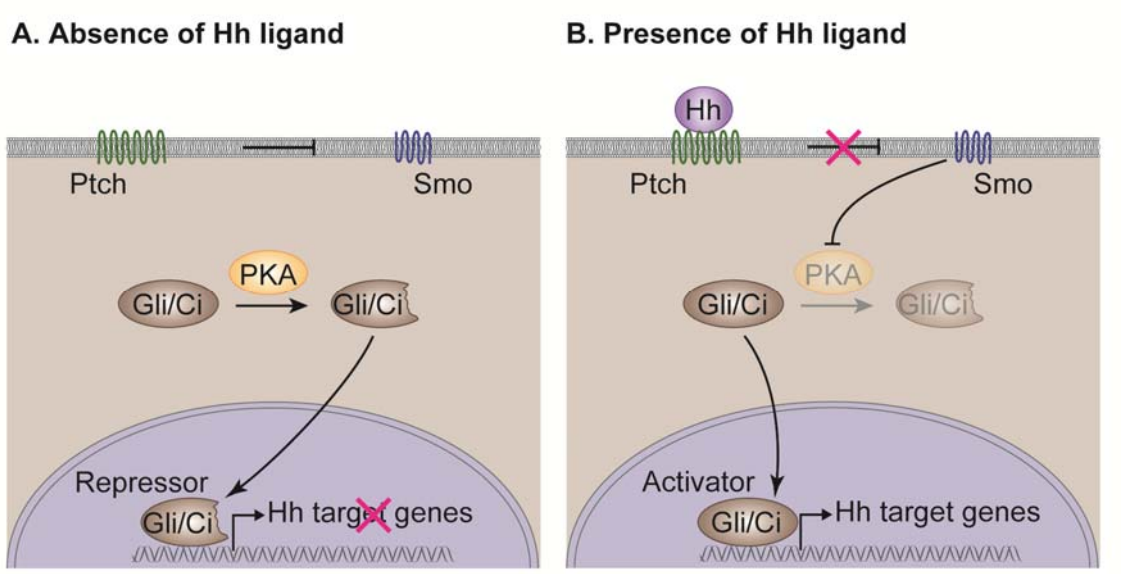

Figure 2. Hedgehog signal transduction pathway.

(A) In the absence of the Hedgehog (Hh) ligand, the downstream transcription factor Gli/Ci is cleaved to its repressor form through PKA-dependent phosphorylation. (B) When Hh ligand binds to Patched (Ptch), the conformation of Ptch is altered, releasing the inhibition of Smoothened (Smo). Smo then inactivates PKA, and Gli/Ci is translocated into the nucleus and activates the transcription of Hh target genes.

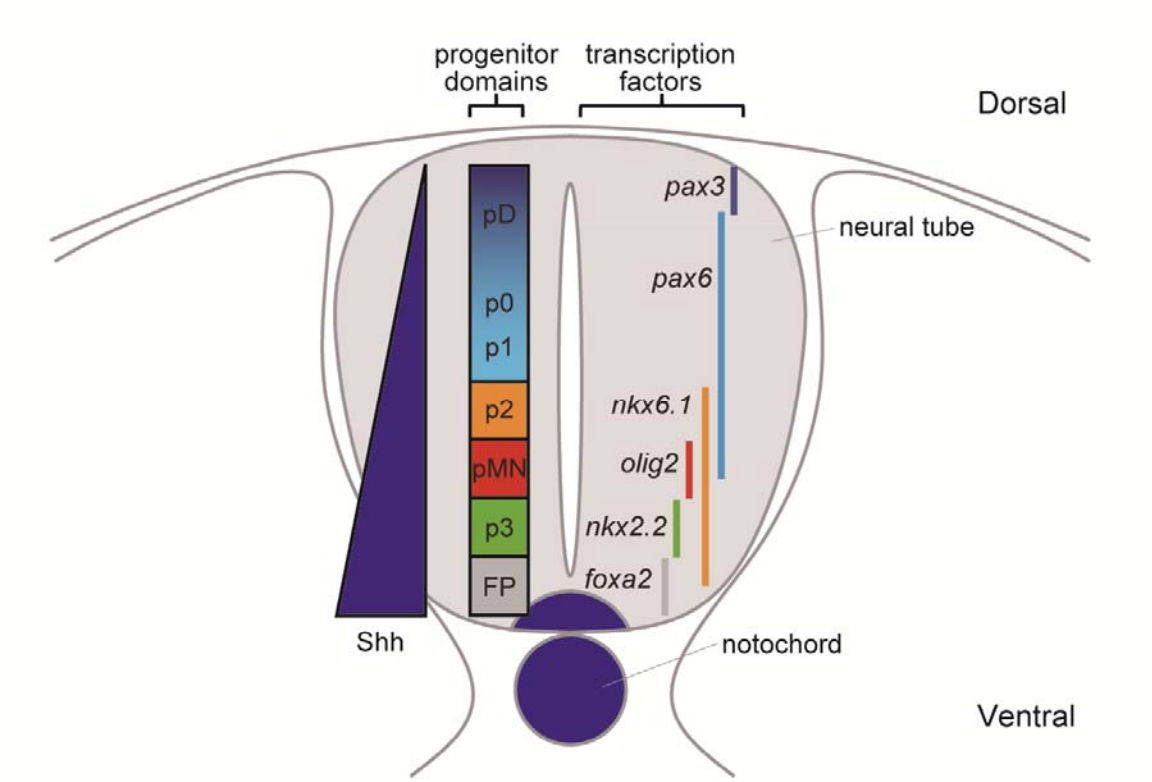

Figure 3. Schematic view of neural tube patterning by Shh concentration gradient.

In the neural tube, Sonic hedgehog (Shh) ligand forms a dorso-ventral gradient from its source, notochord and floorplate. The specific genes for the progenitor domains are expressed in a Shh-ligand concentration dependent manner.

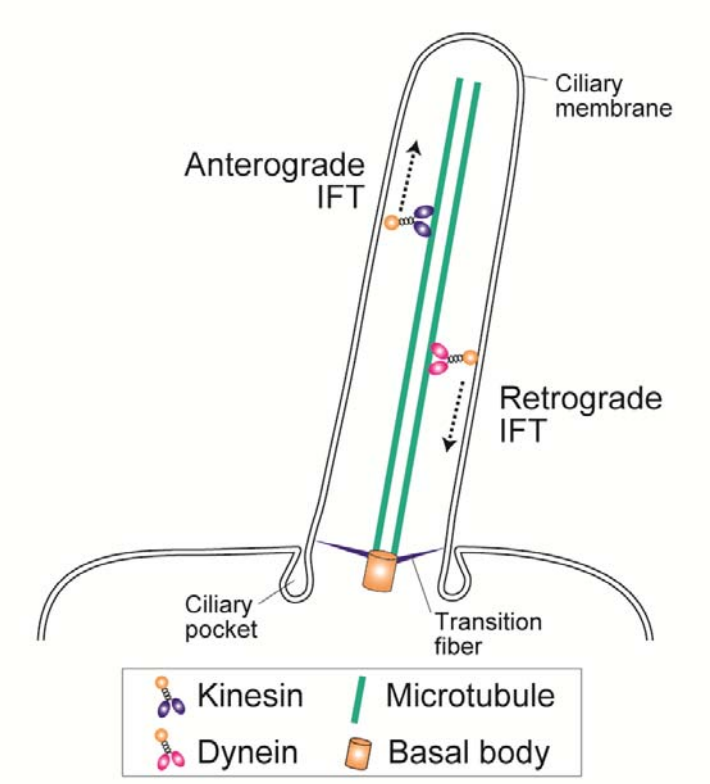

Figure 4. The formation and maintenance of cilia mediated by the intraflagellar transport.

A cilium is a microtubule-based organelle, arise from a basal body anchored to the base of cilia by transition fibers. Ciliary proteins and membrane receptors are delivered by an intraflagellar transport machinery along the ciliary axoneme (microtubule). The anterograde transport, from the basal to tip, is powered by the kinesin, and the retrograde transport, from the tip to the basal, by the cytoplasmic dynein. Most of cilia

have a ciliary pocket at the base, distinguished from the microvilli, which is an actin-based cellular projection and narrower than the cilium.

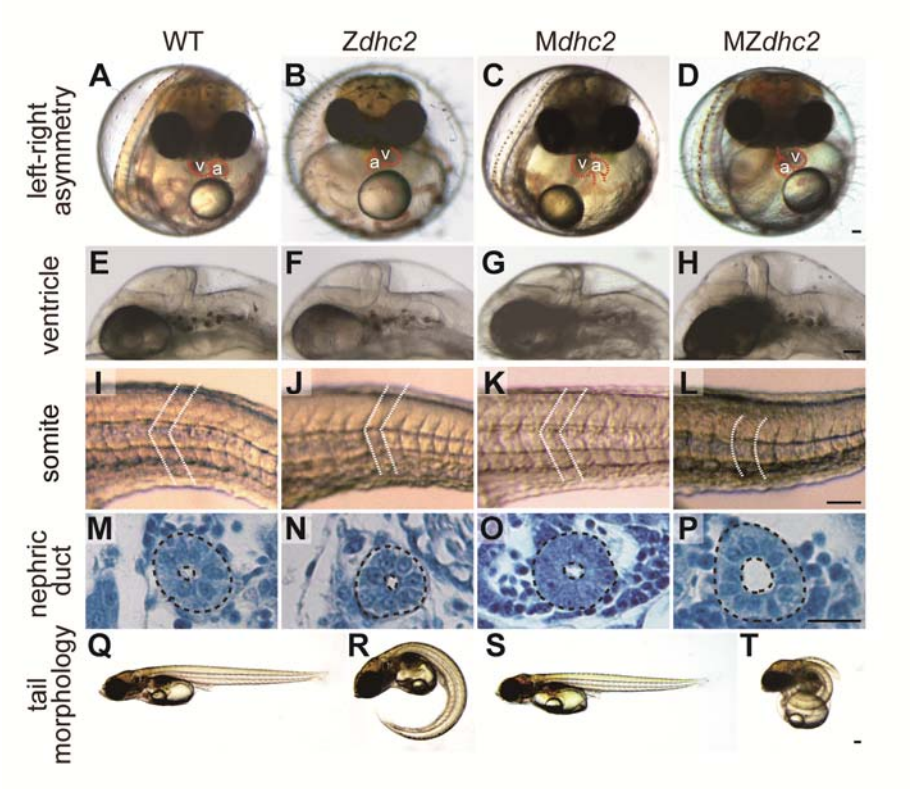

Figure 5. Morphological phenotypes of *aA90*/*dhc2* mutants.

(A-D) Frontal views of the heart at 6 days post fertilization (dpf). In wild type (WT) embryos, the ventricle of the heart positions to their right side and the atrium to the left. Conversely, in zygotic mutants of *dhc2* (*Zdhc2*) and maternal-zygotic mutants of *dhc2* (M*Zdhc2*), the ventricle of the heart positions to their left and the atrium to the right. **(E-L)** Lateral views of the ventricle of the brain (E-H) and the somite (I-L) at 3 dpf. M*Zdhc2* showed enlarged brain ventricles (H) and U-shaped somites (L) instead of chevron-shaped ones (I-K). **(M-T)** Transverse section of nephric duct (M-P) and tail

morphology at 7 dpf (Q-T). MZ*dhc2* embryos exhibited expanded nephric ducts (P). Severe ventral curvature was observed in MZ*dhc2* (T), compared with its zygotic mutants (R). v, ventricle; a, atrium. Scale bars: 100 μm in D, H, L, P; 200 μm in T.

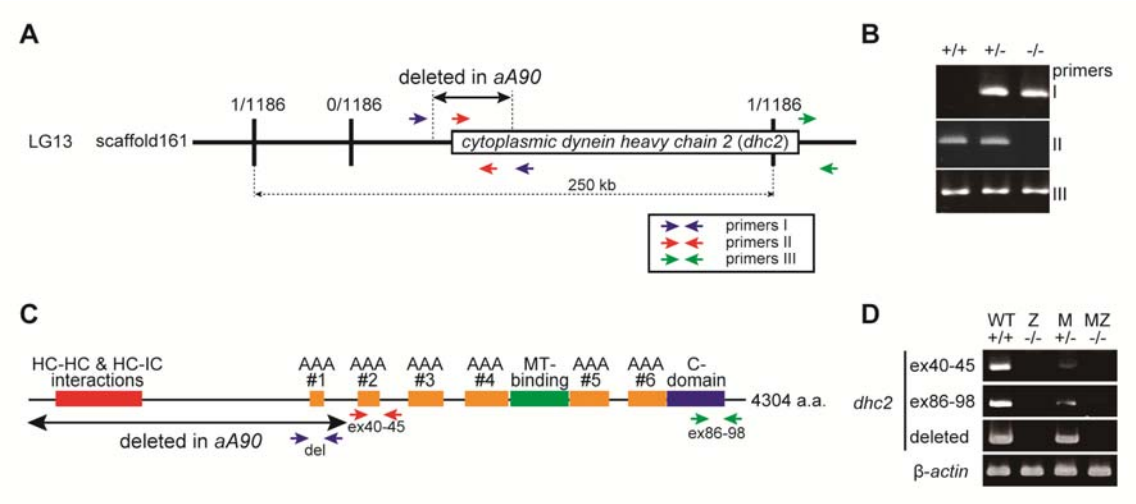

Figure 6. The medaka *aA90*/*dhc2* lacks essential domains of the *dhc2* gene.

(A) Positional cloning of the *aA90* mutation in linkage group (LG) 13. The number of recombinants at each marker is shown. *aA90*/*dhc2* has a 37.7 kb deletion in the *dhc2* locus including the start codon. Colored arrows (blue, red and green) indicates the position of primers used for genotyping described in Fig. 6B.

(B) Genotyping for *aA90*/*dhc2*. The primers for PCR detection were described in arrows of Fig. 6A and listed in Table 2. In *aA90*/*dhc2* mutants, the aberrant product (+/- and -/-, top panel) and the loss of the product (-/-, middle panel) were detected by genomic PCR.

(C) Schematic diagrams of Dhc2 protein expressed in wild-type and the deleted region in mutants. The mutant lacks the heavy chain (HC)-HC and the HC-Intermediate chain interaction domain and the AAA ATPase domain of Dhc2. Colored arrows indicates the primer set for the analysis of *dhc2* expression, described in Fig. 6D. HC, heavy chain; IC, intermediate chain; MT, microtubule; a.a., amino acids.

(D) Expression analysis of *dhc2* at 6 dpf by RT-PCR using primers described in Fig. 6C (arrows) and listed in Table 2. The *dhc2* expression was diminished in homozygous *aA90*/*dhc2* mutants (-/-).

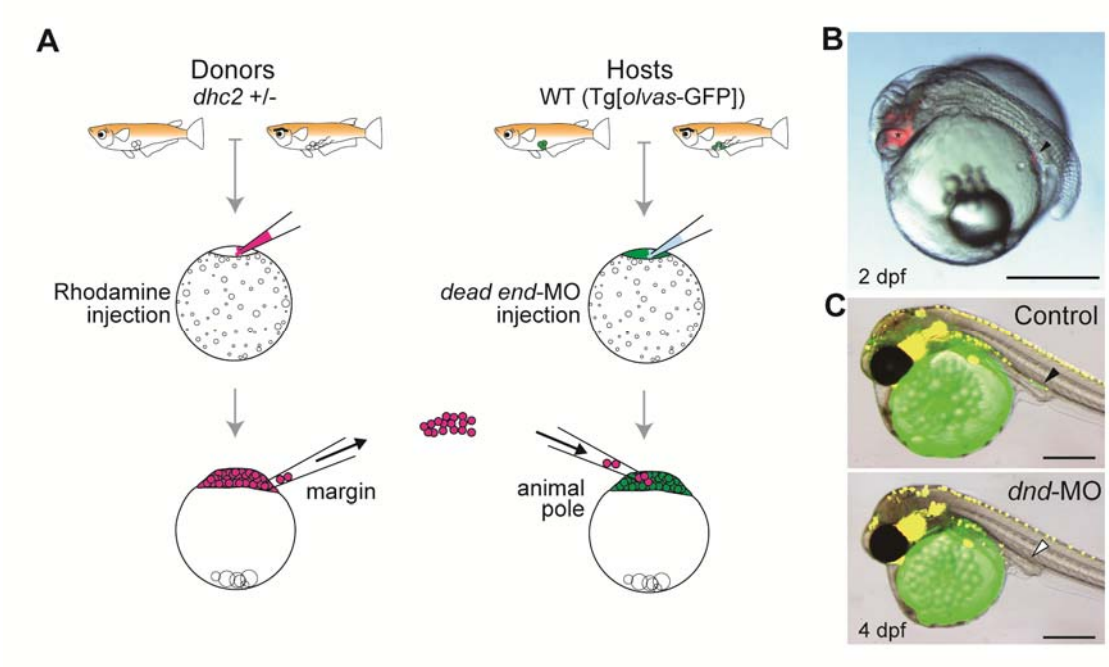

Figure 7. Generation of Maternal-Zygotic *dhc2* mutant (MZ*dhc2*).

Germ-line replacement strategy using the rhodamine-dextran labeling technique. **(A)** Overview of transplantation strategy showing the transfer of cells from the margin of rhodamine-dextran-labeled mutant donor embryos into the animal pole of *dead end*-MO injected WT hosts (Tg[*olvas*-GFP], germ cells are labeled with GFP (Tanaka et al., 2001)). Donor embryos are genotyped after transplantation. A morpholino antisense oligonucleotide (Genetools) to *dead end* was complementary to a region covering the splicing site for exon 2 and intron 2, 5'-TGTTCAGAACTGGCCTCTCACCATC-3'.

(B) Chimeric host embryos were screened at 2 dpf for the presence of rhodamine-labeled donor PGCs that had migrated successfully into the gonadal mesoderm (arrowhead). Host embryos also showed somatic contribution of rhodamine-dextran-labeled donor cells to anterior neuroectoderm lineages (*). **(C)** Chimeric host embryos were screened again at 4-6 dpf for the lost of GFP-labeled host PGCs at the dorsal region of the gut (arrowhead). Scale bars: 500 μm in B-C.

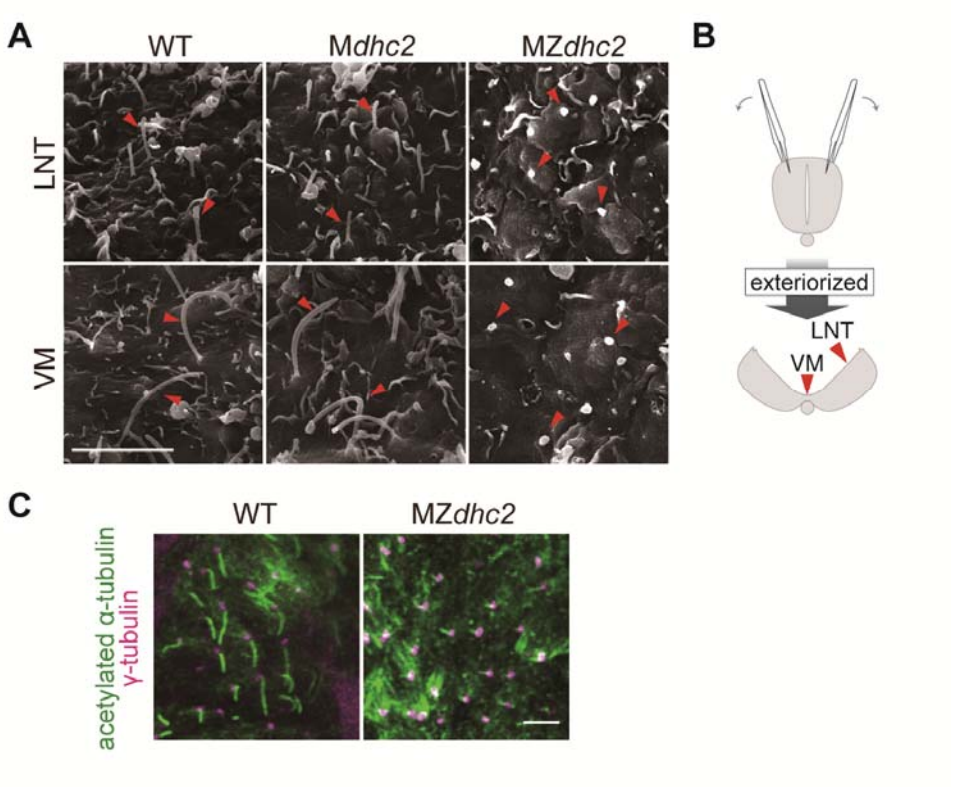

Figure 8. Cilia are shortened in MZ*dhc2*.

(A) SEM analysis of the ventricular surface of the neural tube at 16-somite stage. Cilia were found on the surface of neural epithelial cells (arrowheads). In wild type and M*dhc2*, longer cilia were observed on the floorplate (VM, ventral midline), compared with those on the lateral neural tube (LNT). Cilia in MZ*dhc2* were greatly shortened on both regions. **(B)** Schematic view of opening of the apical surface of neural tube with forceps. **(C)** Medaka MZ*dhc2* mutants have shortened cilia in Kupffer's vesicle. Cilia

were visualized by staining with anti-acetylated α-tubulin antibody (green) and basal bodies were visualized with anti-γ-tubulin antibody (magenta). Scale bars: 5 μm.

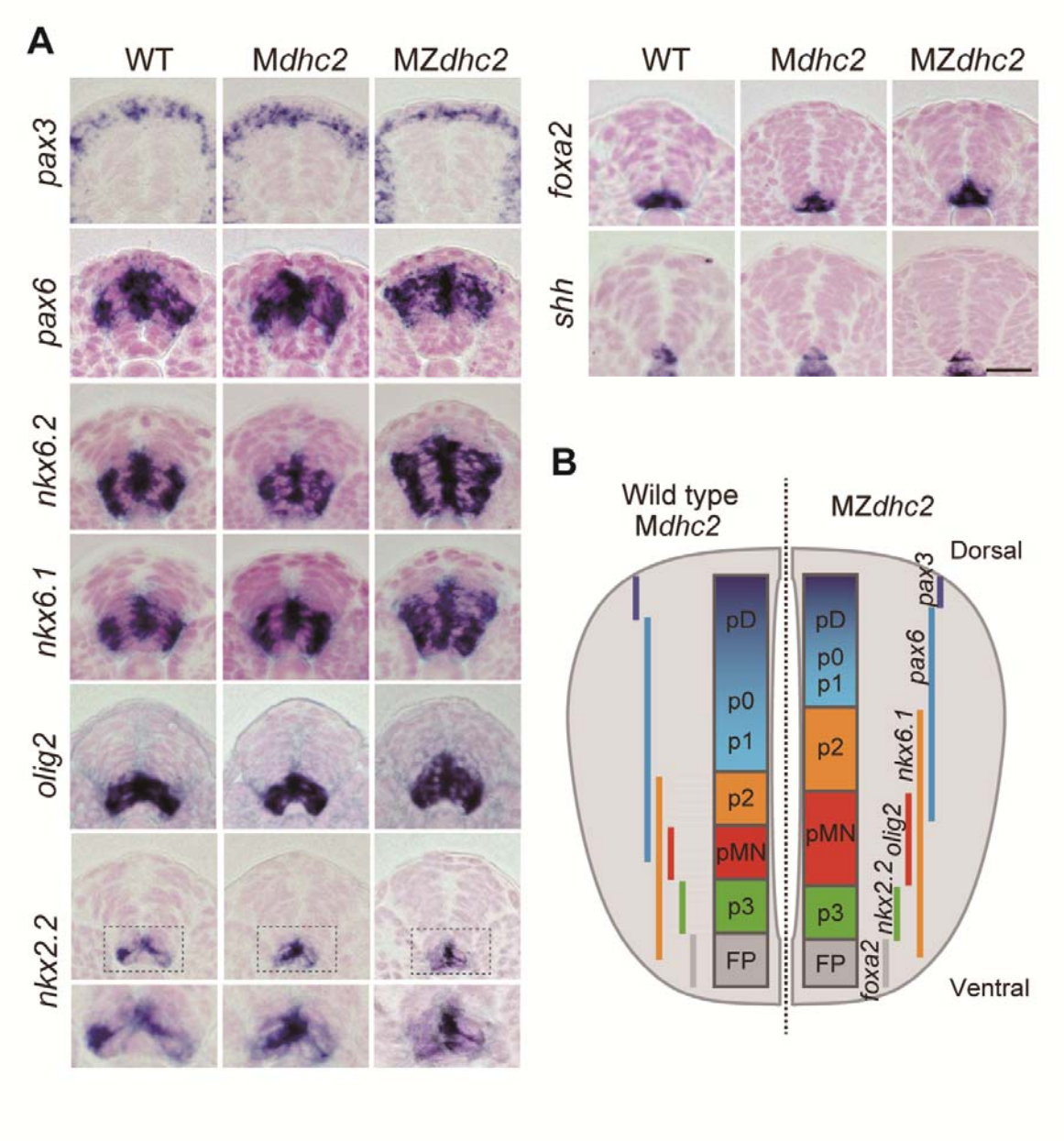

Figure 9. Neural tube patterning in MZ*dhc2* mutants.

(A) Expression of neural tube markers in a cross-sectional view at 16-somite stage (The dashed line in Fig. 10A indicates the section plane). All Hh target genes were expressed in M*Zdhc2*, but *olig2* and *nkx6.1/6.2* expression was dorsally expanded. The lower

panels of *nkx2.2* are the magnified images of the upper panels (dotted line). **(B)** Representation of the size of each progenitor domain along the DV axis in WT, M*dhc2* and MZ*dhc2*. Scale bar represents 20 μm.

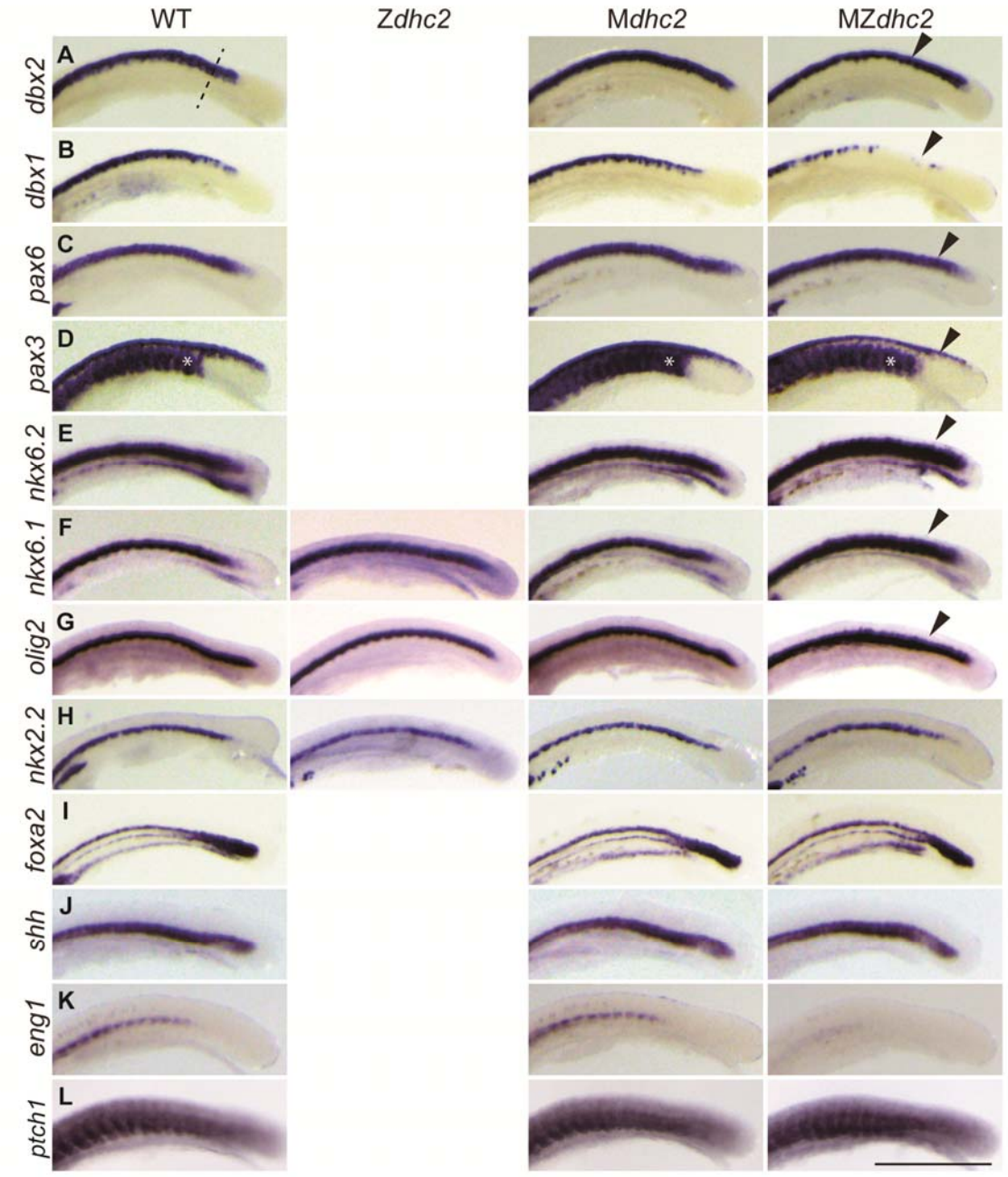

Figure 10. Gross patterning of neural tube and somite in MZ*dhc2* mutant.

(A-J) Expression of neural tube markers in MZ*dhc2* mutant embryos. Wild type, M*dhc2* control medaka embryos and MZ*dhc2* mutants were stained at 16-somite stage for the

expression of *dbx2* (A), *dbx1* (B), *pax3* (C), *pax6* (D), *nkx6.2* (E), *nkx6.1* (F), *olig2* (G), *nkx2.2* (H), *foxa2* (I), *shh* (J), shown in a lateral view. M*Zdhc2* mutants show *shh*, *foxa2* and *nkx2.2* expression (H-J), dorsally expanded expression of *olig2*, *nkx6.1* and *nkx6.2* (E-G; arrowheads), and retracted expression of *dbx* genes, *pax6* and *pax3* (A-D; arrowheads), compared with those expression in the control embryos. * in D indicates somites. Cross-sectional views at the dashed line in A were depicted in Fig. 9A. **(K)** Somite patterning in M*Zdhc2* embryos. Adaxial cells (*engrailed1*-positive cells) were significantly decreased in M*Zdhc2* as compared with control embryos. **(L)** *ptch1* expression in M*Zdhc2* is nearly identical to that in WT. Scale bar: 500 μm.

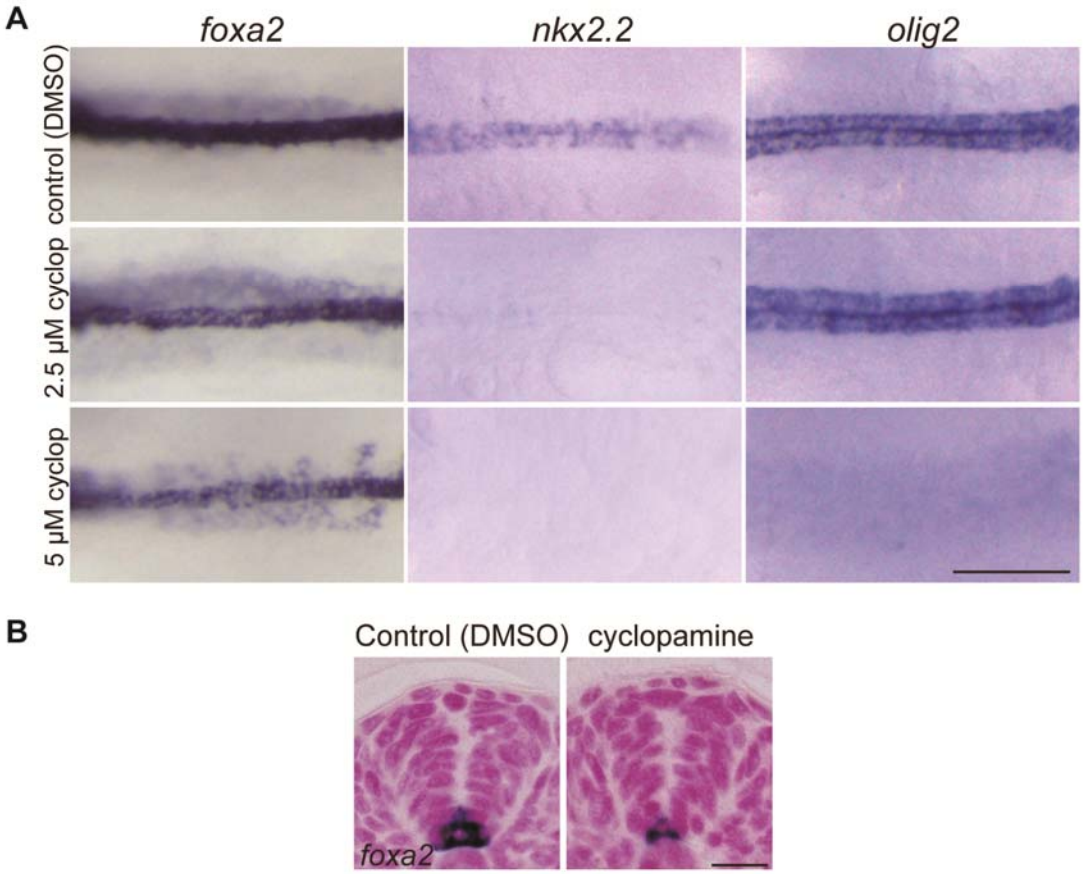

Figure 11. Dose-dependent effects of cyclopamine treatment on the expression of Hh target genes.

(A) *foxa2*, *nkx2.2* and *olig2* expression in WT embryos treated with DMSO, 2.5 µM and 5 µM cyclopamine (cyclop). **(B)** *foxa2* expression is absent in the lateral FP and only detectable in the medial FP in embryos treated with 5 µM cyclopamine, when compared to the DMSO control. Scale bars: 100 µm in A, 20 µm in B.

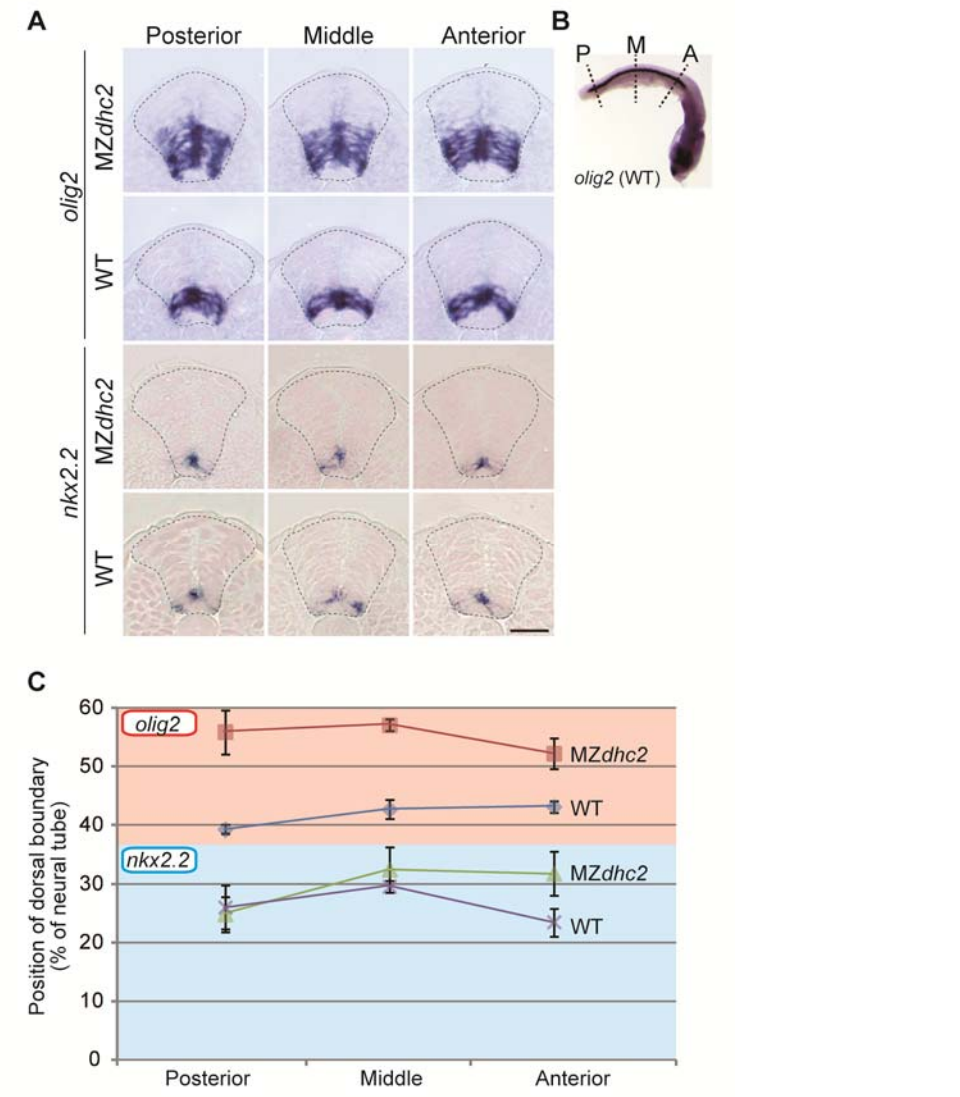

Figure 12. *nkx2.2* and *olig2* expression at three anterior-posterior axis levels.

(A) *nkx2.2* and *olig2* expression at three different anterior-posterior axis levels of 16-somite stage embryos. **(B)** *olig2* expression in WT for indicating the position of anterior (A), middle (M) and posterior (P) level, depicted in A and C. **(C)** Measurement of the dorsal boundary of *nkx2.2* and *olig2* expression at relative distances (percentage

(%) of the neural tube) from the floor plate in WT and MZ*dhc2* of 16-somite stage (n ≥ 3 embryos; mean ± SD). For the representation of the dorsal boundary of *nkx2.2* and *olig2* expression in same graph, blue shade is for *nkx2.2* and red shade is for *olig2* expression. The *olig2* boundary in mutant embryos is significantly different from WT counterparts (p values from Student's t test: Anterior, $p < 0.05$; Middle, $p < 0.0005$; Posterior, $p < 0.005$). Scale bar represents 20 μm.

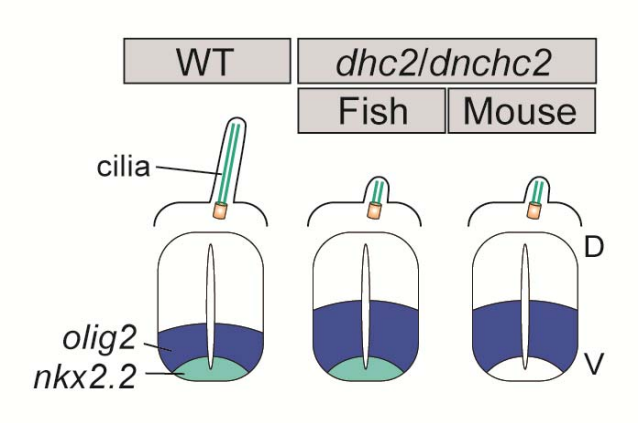

Figure 13. A schematic drawing explaining the similarities and differences in ciliary and neural tube phenotypes between fish and mouse *dhc2*/*dnchc2* mutants.

Ciliary phenotypes and dorsal expansion of *olig2* domain in MZ*dhc2* mutants are nearly identical to those in mouse mutant, but *nkx2.2* expression was reported to be lost in mouse mutant (Huangfu and Anderson, 2005; May et al., 2005). D, dorsal; V, ventral.

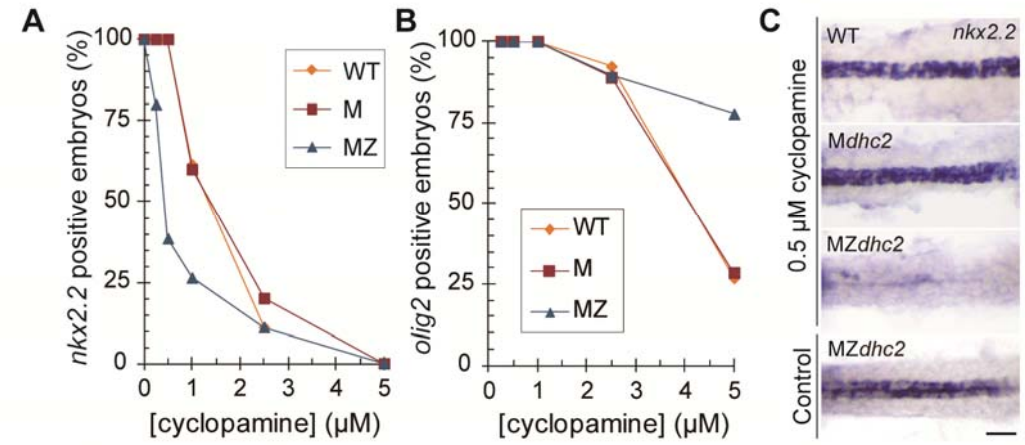

Figure 14. Hh signaling activity is partially defective in MZ*dhc2* mutants.

(A-B) The percentage of *nkx2.2* (A), *olig2* (B) positive embryos with the graded series of cyclopamine treatment (Sample numbers are indicated in Table 4). **(C)** Dorsal view of *nkx2.2* expression in 0.5 μM cyclopamine treated and control (DMSO-treated) embryos. Scale bars: 100 μm in C.

Figure 15. MZ*dhc2* is sensitive to dnPKA.

dnPKA mRNA injected MZ*dhc2* exhibited expanded *nkx2.2* expression (n=19/24, arrowhead), consistent with *dnPKA* mRNA injected-WT (n=22/24, arrowhead) and M*dhc2* embryos (n=17/20, arrowhead), compared with Control (WT) embryos. Scale bar: 500 μm

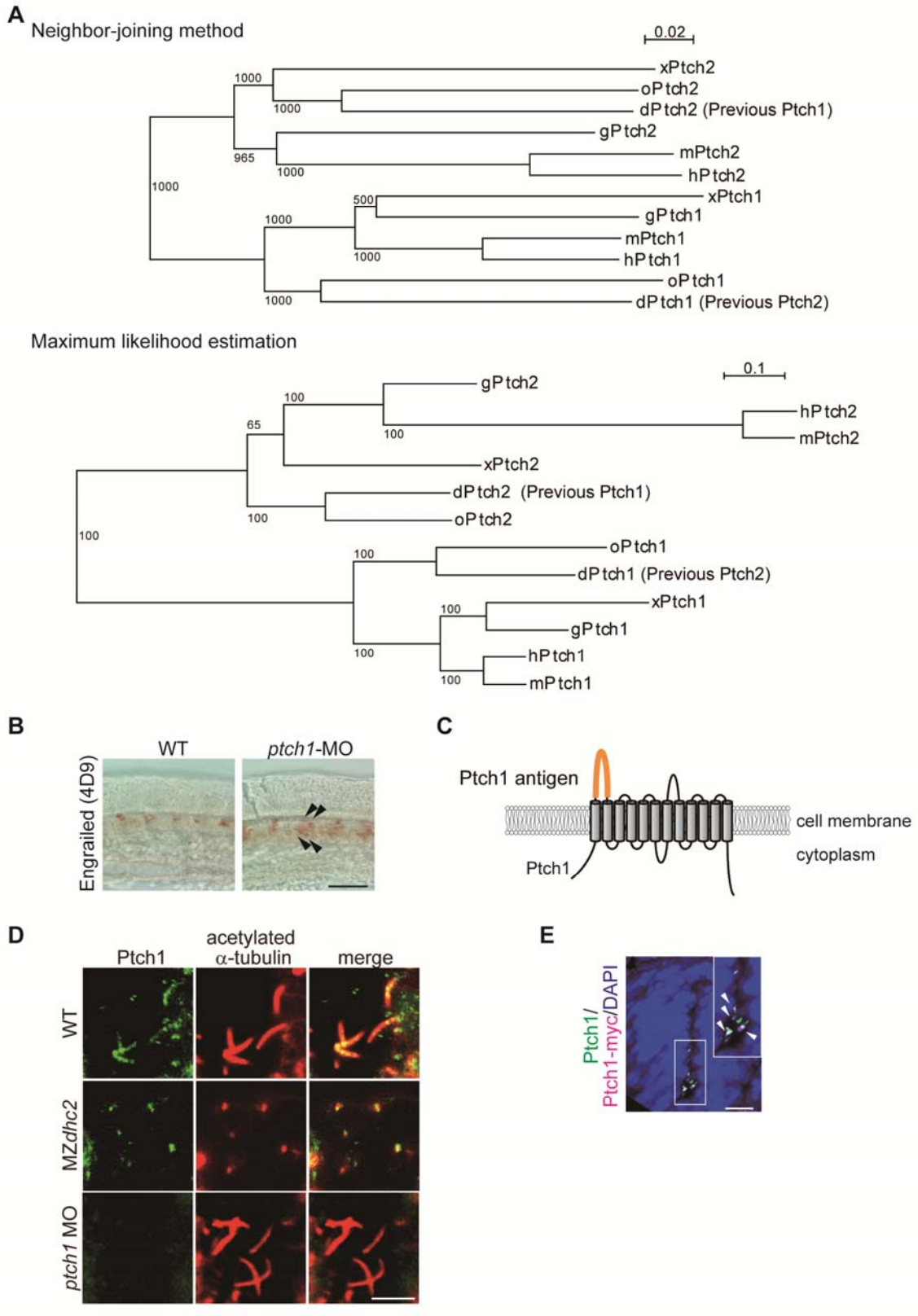
A
Neighbor-joining method
0.02
xPtch2
oPtch2
dPtch2 (Previous Ptch1)
gPtch2
mPtch2
hPtch2
xPtch1
gPtch1
mPtch1
hPtch1
oPtch1
dPtch1 (Previous Ptch2)
1000
1000
965
1000
1000
500
1000
1000
1000
Maximum likelihood estimation
0.1
gPtch2
hPtch2
mPtch2
xPtch2
dPtch2 (Previous Ptch1)
oPtch2
oPtch1
dPtch1 (Previous Ptch2)
xPtch1
gPtch1
hPtch1
mPtch1
100
65
100
100
100
100
100
100
100
B
WT
ptch1-MO
Engrailed (4D9)
C
Ptch1 antigen
cell membrane
cytoplasm
Ptch1
D
Ptch1
acetylated α-tubulin
merge
WT
MZdhc2
ptch1 MO
E
Ptch1/
Ptch1-myc/DAPI

Figure 16. Ptch1 is localized to the cilia in medaka fish.

(A) Phylogenetic trees showing the relationship between Patched proteins across vertebrates based on neighbor-joining method using ClustalX and maximum likelihood estimation using RAxML. o, *Oryzias latipes* (medaka); g, *Gallus gallus*; h, *Homo sapiens*; m, *Mus musculus*; x, *Xenopus tropicalis*; d, *Danio rerio*. In the both methods, medaka Ptch1 is the homologue of mammalian Ptch1, not Ptch2. All sequences are obtained from Ensembl Web site and the accession numbers are listed on Table 3. **(B)** Injection of *ptch1*-morpholino antisense oligo for splicing blocking (intron 5 and exon 6) (5'-CCCCTACCTCTGTAAAGTTAATTAC-3') induced ectopic Hh-dependent muscle pioneer (Eng+ cells, lateral view, arrowheads), visualized by staining with anti-Engrailed antibody (4D9). **(C)** The recombinant protein of His-tagged N-terminal (169-405; Ptch1- His) polypeptides of medaka Ptch1 (orange lined) were expressed using pET24a vector and the polypeptides were used for immunization of rabbits. **(D)** Ptch1 were visualized by staining with anti-medaka Ptch1 antibody (green) and cilia were visualized with anti-acetylated α-tubulin antibody (red). Ptch1 morpholino oligo injected embryos (*ptch1* MO) had no Ptch1 positive signals at 16-somite stage. **(E)**

Ptch1-myc (magenta) was specifically localized to cilia in neural tube and the signals are well merged with anti-Ptch1 antibody signals (green) in a cross-sectional view at 16-somite stage (arrowheads). The inset on the right side is a high magnified image of the square region. Scale bars: 50 μm in B, 5 μm in D, 10 μm in E.

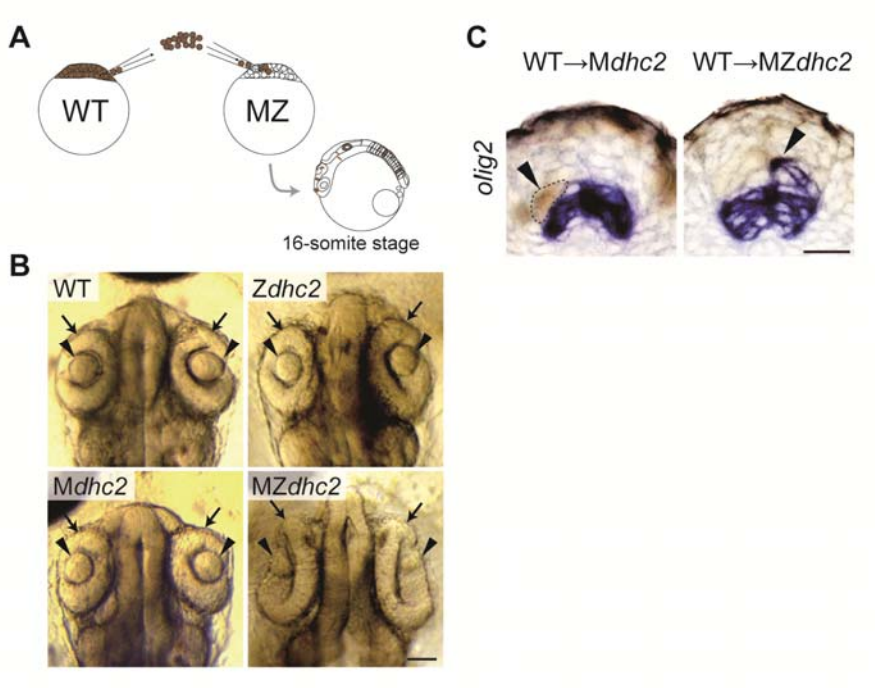

Figure 17. Ectopic *olig2* expression of WT cells in the dorsal region of MZ*dhc2* neural tube.

(A) Schematic view of the transplantation of biotin-injected WT cells (brown colored) into M*dhc2* (control) and MZ*dhc2* embryos. **(B)** Dorsal views of the eyes in WT, *Zdhc2*, M*dhc2* and MZ*dhc2* at 16-somite stage. Optic cup and lens formation were significantly defected in MZ*dhc2*, as compared with WT, *Zdhc2* and M*dhc2*. Arrows indicate optic cup and arrowheads indicate lens. **(C)** *olig2* expression in the transplanted embryos. Ectopic *olig2* expression (purple) of WT cells (brown) was observed in the dorsal

region of M*Zdhc2* neural tube (arrowhead, right panel), not in that of M*dhc2* one (arrowhead, left panel). Scale bars: 100 μm in B, 20 μm in C.

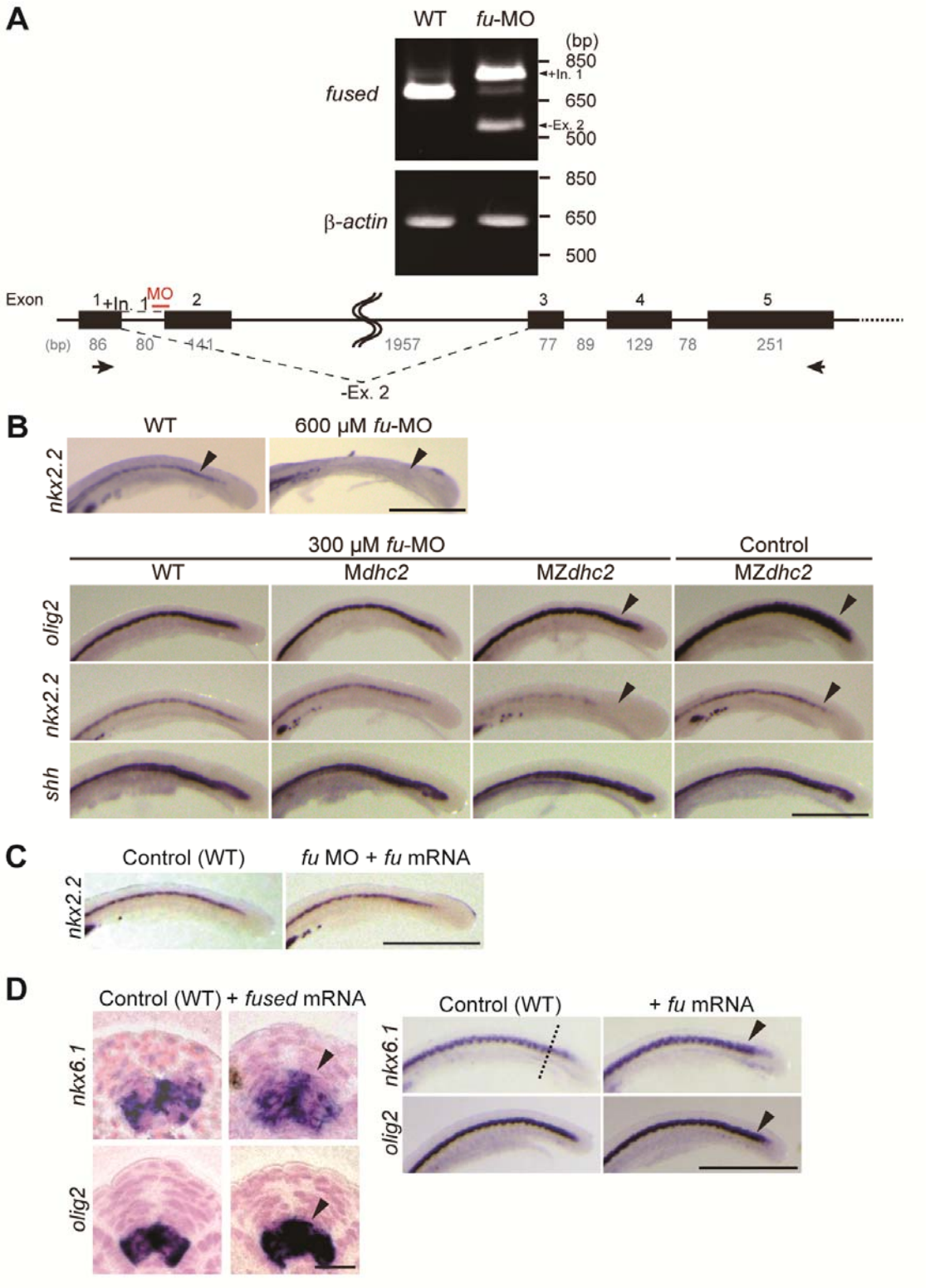
A
WT
fu-MO
(bp)
fused
850
+In. 1
650
-Ex. 2
500
β-actin
850
650
500
Exon
1+In. 1
MO
2
3
4
5
(bp)
86
80
141
1957
77
89
129
78
251
-Ex. 2
B
WT
600 μM fu-MO
nkx2.2
300 μM fu-MO
Control
WT
Mdhc2
MZdhc2
MZdhc2
olig2
nkx2.2
shh
C
Control (WT)
fu MO + fu mRNA
nkx2.2
D
Control (WT) + fused mRNA
nkx6.1
olig2
Control (WT)
+ fu mRNA
nkx6.1
olig2

Figure 18. *fused* is required for Hh signaling in medaka fish.

(A) Knockdown of *fu* was performed using the morpholino-oligonucleotide (MO) for splice blocking (5'-CAACCACCTTATTGACGACAAAACA-3'). Diagram of altered *fu* splicing in morphants of *fu*-i1e2 inserts intron 1 (+In. 1), resulting in an out-of-frame truncation of the *fu* protein, and splices exon 2 to a cryptic acceptor in exon 3 (- Ex. 2), causing an out-frame mutation of *fu*. The effect of the splice-blocking MO was verified by RT-PCR from 20 embryos total RNA (16-somite stage). The positions of primers for checking the effect of MO were indicated in A (arrows) and listed in Table 2. MO caused splice-blocking effectively. **(B)** *nkx2.2*, *olig2* and *shh* expression in *fu*-MO injected embryos. *nkx2.2* expression was almost diminished in 600 μM *fu*-MO injected WT embryos (arrowhead) and greatly reduced in 300 μM *fu*-MO injected MZ*dhc2* embryos (arrowhead). The dorsal expanded expression of *olig2* was rescued in 300 μM *fu*-MO injected MZ*dhc2* embryos (arrowhead). **(C)** *fu* mRNA injection rescued *nkx2.2* expression in *fu*-MO injected embryos. **(D)** *fu* overexpression induced ectopic *nkx6.1* and *olig2* expression (arrowheads) in a cross-section view and a lateral view (the dashed line indicates the section plane).

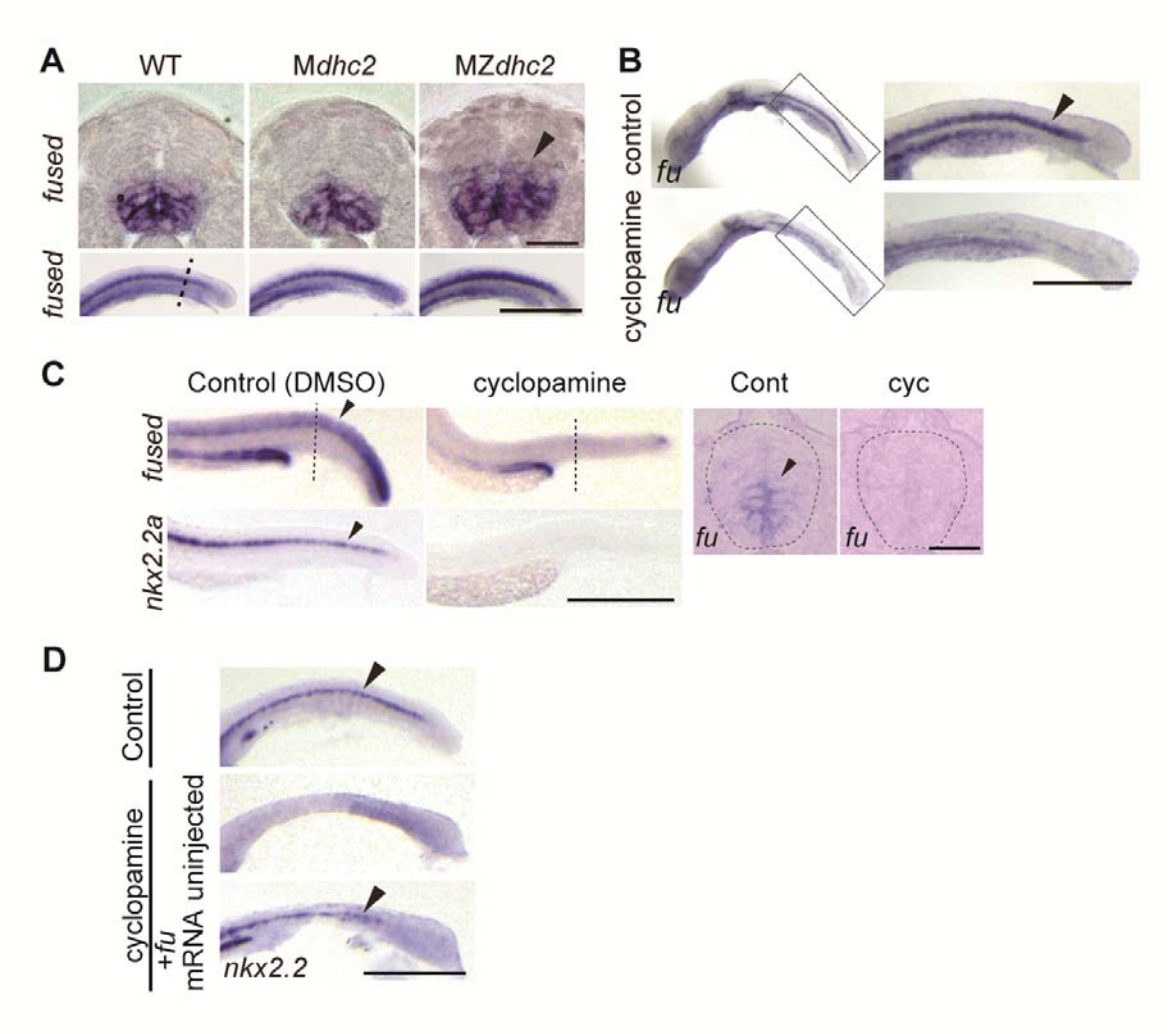

Figure 19. *fused* expression pattern in medaka and zebrafish, and *fused* augments Hh signaling in medaka.

(A) *fu* expression in a cross-sectional view and a lateral view (the dashed line indicates the section plane). *fused* expression was ventrally restricted. Dorsally expanded expression of *fu* was observed in MZ*dhc2* (arrowhead). **(B)** *fu* expression (arrowhead) in the neural tube was lost in 5 μM cyclopamine-treated embryos. Black lines mark the

magnified areas, depicted in the right panel. **(C)** *fu* expressed in a Hedgehog-dependent fashion also in zebrafish. The embryos treated with 100 μM cyclopamine did not express *fused* or *nkx2.2a* (a Hh target gene). Arrowheads indicate the expression in the neural tube. The dashed line indicates the section plane. **(D)** The loss of *nkx2.2* expression in 2.5 μM cyclopamine-treated embryos (n=13/14) was rescued by overexpression of *fused* (n=12/18, arrowhead). Scale bars: 500 μm in A (lower panel), B, C (left panel), D; 20 μm in A (upper panel), C (right panel).

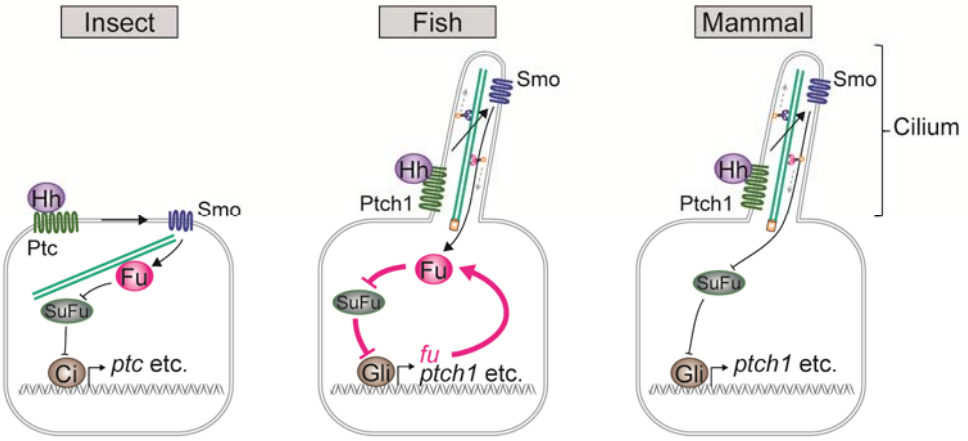

Figure 20. Proposed model of the distinct features of Hh signal transduction in insect, fish and mammal.

fu is expressed in a Hedgehog-dependent fashion and is also one of the components of the Hedgehog pathway in fish. Fused negatively regulates Suppressor of Fused (SuFu), which is a negative regulator of Gli/Ci in Hh signaling. The transcription of *fused* in fish could lead to Hh activation. This positive-feedback loop amplifies Hedgehog pathway in fish downstream of cilia.

Tables

Table 1. Defects in heart asymmetry in *dhc2* mutant embryos and morphants

Genotype	n	Correct (%)	Reversed (%)
Wild type	110	99.1	0.9
Z*dhc2*	294	76.2	23.8
dhc2 MO*	108	77.8	22.2
M*dhc2*	82	100	0
MZ*dhc2*	128	46.9	53.1

* *dhc2*-Met MO, 5'-AAATGCGGCAGACTCGCAGTTTTAC-3’

Table 2. Primers used in this study

Genotype	Forward (5' to 3')	Reverse (5' to 3')
primers I	CCCGCTGAGTTTAGAGACTATTG	GTGGGAAGTGTACACCTTCATAAT
primers II	TTCTATGGGTGATGCCACTTTC	GGAAATCTGATACAACCCCAGC
primers III	CTCAAAGTGAGCTTTTGGCTCAAGTATT	ACTGTAGAAGATGGGACACGAAGAAAAG

Probe*	Forward (5' to 3')	Reverse (5' to 3')
nkx2.2	TCGTTGACCAACACAAAGACGG	CCAAGTCCTGAGCTTTAAGAGTGTG
olig2	ATACAAGTCGTGTGTCAAGCAGACC	TGAGAAGTCCGTGATGGGGTC
fused	TTCAGTAAAAACGCGTGAGC	AACACGTTTGTGTCCGACAG
nkx6.1	TCTTCTGGCCGGGAGTCATG	AAGTGCTTTACATGAAGCTGCG
nkx6.2	ATGGAAGCTAACCGGCAGAG	CACTTGGTCCTCCGGTTCTG
pax3	CAGGAGGTTTACCAAGAATGATG	AAGACTGAGTACTGGGCAGAGTG
dbx1	AAGAAGCGGTTCCTGATTTCTC	CTCATTCTTTCTCCTCCCAACTC
dbx2	CTCCTGCTCTGCCAGGTTTTG	CACTGGTGTGATTGTGTGACAG
eng1	AACCACCAACTTTTTCATCGAC	ATCTGGGACTCGTTCAGGTG
zebrafish *nkx2.2a*	GCACTCCTTACTTTCATTTGG	CGTATAACACGAAGGACAAAAG
zebrafish *fused*	GGAGAAAACGGTCTAAGTTATG	ATCAGAACTCCATCTGCAAC

**shh* (AB007129) and *foxa2* (AB001572) were kindly provided by Dr. K. Araki; *pax6* were by Dr. A. Kawakami.

RT-PCR	Forward (5' to 3')	Reverse (5' to 3')
fused	ATGAATTCCTATCACGTCTTG	ATGCAGTTATCACTCATTGTGTC
β-*actin*	GATGAAGCCCAGAGCAAGAG	AGGAAGGAAGGCTGGAAGAG
dhc2 (ex40-45)	GTGCAAGCACTGAGGCTC	CACTAGACTAGTTTCCACCACAAAG
dhc2 (ex86-98)	CTTTGTCCACGGCCTGTTC	CTGTTTGAGAAAAAGAGCAGCTC
dhc2 (del)	GTTGAGGTGTGGTTAGGAGAGC	TGGTTTGCTCATGGCTACG

Table 3. Accession numbers used to create the phylogenetic trees depicted in Fig. 16A.

	Ptch1	Ptch2
Oryzias latipes	ENSORLG00000004345	ENSORLG00000016137
Gallus gallus	ENSGALG00000012620	ENSGALG00000010133
Homo sapiens	ENSG00000185920	ENSG00000117425
Mus musculus	ENSMUSG00000021466	ENSMUSG00000028681
Xenopus tropicalis	ENSXETG00000014834	ENSXETG00000018892
Danio rerio	ENSDARG00000016404	ENSDARG00000055026

Table 4. Number of samples to examine Hh activity with the graded series of cyclopamine treatment depicted in Fig. 14A-B.

cyclopamine (nM)		250	500	1000	2500	5000
nkx2.2	Wild type	20	23	26	18	17
	M*dhc2*	18	19	20	20	18
	MZ*dhc2*	20	26	19	18	16
olig2	Wild type	17	22	19	26	26
	M*dhc2*	16	22	18	18	14
	MZ*dhc2*	15	12	13	19	18

References

Aanstad, P., Santos, N., Corbit, K. C., Scherz, P. J., Trinh le, A., Salvenmoser, W., Huisken, J., Reiter, J. F. and Stainier, D. Y. (2009). The extracellular domain of Smoothened regulates ciliary localization and is required for high-level Hh signaling. *Curr Biol* **19**, 1034-1039.

Balaskas, N., Ribeiro, A., Panovska, J., Dessaud, E., Sasai, N., Page, K. M., Briscoe, J. and Ribes, V. (2012). Gene regulatory logic for reading the Sonic Hedgehog signaling gradient in the vertebrate neural tube. *Cell* **148**, 273-284.

Ben, J., Elworthy, S., Ng, A. S., van Eeden, F. and Ingham, P. W. (2011). Targeted mutation of the talpid3 gene in zebrafish reveals its conserved requirement for ciliogenesis and Hedgehog signalling across the vertebrates. *Development* **138**, 4969-4978.

Chamberlain, C. E., Jeong, J., Guo, C., Allen, B. L. and McMahon, A. P. (2008). Notochord-derived Shh concentrates in close association with the apically positioned basal body in neural target cells and forms a dynamic gradient during neural patterning. *Development* **135**, 1097-1106.

Chen, M. H., Gao, N., Kawakami, T. and Chuang, P. T. (2005). Mice deficient in the fused homolog do not exhibit phenotypes indicative of perturbed hedgehog signaling during embryonic development. *Mol Cell Biol* **25**, 7042-7053.

Ciruna, B., Weidinger, G., Knaut, H., Thisse, B., Thisse, C., Raz, E. and Schier, A. F. (2002). Production of maternal-zygotic mutant zebrafish by germ-line replacement. *Proc Natl Acad Sci U S A* **99**, 14919-14924.

Dessaud, E., McMahon, A. P. and Briscoe, J. (2008). Pattern formation in the vertebrate neural tube: a sonic hedgehog morphogen-regulated transcriptional network. *Development* **135**, 2489-2503.

Dessaud, E., Ribes, V., Balaskas, N., Yang, L. L., Pierani, A., Kicheva, A., Novitch, B. G., Briscoe, J. and Sasai, N. (2010). Dynamic assignment and maintenance of positional identity in the ventral neural tube by the morphogen sonic hedgehog. *PLoS Biol* **8**, e1000382.

Dishinger, J. F., Kee, H. L., Jenkins, P. M., Fan, S., Hurd, T. W., Hammond, J. W., Truong, Y. N., Margolis, B., Martens, J. R. and Verhey, K. J. (2010). Ciliary entry of the

kinesin-2 motor KIF17 is regulated by importin-beta2 and RanGTP. *Nat Cell Biol* **12**, 703-710.

Eggenschwiler, J. T. and Anderson, K. V. (2007). Cilia and developmental signaling. *Annu Rev Cell Dev Biol* **23**, 345-373.

Goetz, S. C. and Anderson, K. V. (2010). The primary cilium: a signalling centre during vertebrate development. *Nat Rev Genet* **11**, 331-344.

Huang, P. and Schier, A. F. (2009). Dampened Hedgehog signaling but normal Wnt signaling in zebrafish without cilia. *Development* **136**, 3089-3098.

Huangfu, D. and Anderson, K. V. (2005). Cilia and Hedgehog responsiveness in the mouse. *Proc Natl Acad Sci U S A* **102**, 11325-11330.

---- (2006). Signaling from Smo to Ci/Gli: conservation and divergence of Hedgehog pathways from Drosophila to vertebrates. *Development* **133**, 3-14.

Huangfu, D., Liu, A., Rakeman, A. S., Murcia, N. S., Niswander, L. and Anderson, K. V. (2003). Hedgehog signalling in the mouse requires intraflagellar transport proteins. *Nature* **426**, 83-87.

Ishikawa, Y. (1996). A recessive lethal mutation, tb, that bends the midbrain region of the neural tube in the early embryo of the medaka. *Neurosci Res* **24**, 313-317.

Iwamatsu, T. (2004). Stages of normal development in the medaka Oryzias latipes. *Mech Dev* **121**, 605-618.

Jeong, J. and McMahon, A. P. (2005). Growth and pattern of the mammalian neural tube are governed by partially overlapping feedback activities of the hedgehog antagonists patched 1 and Hhip1. *Development* **132**, 143-154.

Kee, H. L., Dishinger, J. F., Blasius, T. L., Liu, C. J., Margolis, B. and Verhey, K. J. (2012). A size-exclusion permeability barrier and nucleoporins characterize a ciliary pore complex that regulates transport into cilia. *Nat Cell Biol* **14**, 431-437.

Kimmel, C. B., Ballard, W. W., Kimmel, S. R., Ullmann, B. and Schilling, T. F. (1995). Stages of embryonic development of the zebrafish. *Dev Dyn* **203**, 253-310.

Kuzhandaivel, A., Schultz, S. W., Alkhori, L. and Alenius, M. (2014). Cilia-mediated hedgehog signaling in Drosophila. *Cell Rep* **7**, 672-680.

May, S. R., Ashique, A. M., Karlen, M., Wang, B., Shen, Y., Zarbalis, K., Reiter, J., Ericson, J. and Peterson, A. S. (2005). Loss of the retrograde motor for IFT disrupts localization of Smo to cilia and prevents the expression of both activator and repressor functions of Gli. *Dev Biol* **287**, 378-389.

McMahon, A. P., Ingham, P. W. and Tabin, C. J. (2003). Developmental roles and clinical significance of hedgehog signaling. *Curr Top Dev Biol* **53**, 1-114.

Merchant, M., Evangelista, M., Luoh, S. M., Frantz, G. D., Chalasani, S., Carano, R. A., van Hoy, M., Ramirez, J., Ogasawara, A. K., McFarland, L. M., et al. (2005). Loss of the serine/threonine kinase fused results in postnatal growth defects and lethality due to progressive hydrocephalus. *Mol Cell Biol* **25**, 7054-7068.

Nonaka, S., Tanaka, Y., Okada, Y., Takeda, S., Harada, A., Kanai, Y., Kido, M. and Hirokawa, N. (1998). Randomization of left-right asymmetry due to loss of nodal cilia generating leftward flow of extraembryonic fluid in mice lacking KIF3B motor protein. *Cell* **95**, 829-837.

Nusslein-Volhard, C. and Wieschaus, E. (1980). Mutations affecting segment number and polarity in Drosophila. *Nature* **287**, 795-801.

Ocbina, P. J., Eggenschwiler, J. T., Moskowitz, I. and Anderson, K. V. (2011). Complex interactions between genes controlling trafficking in primary cilia. *Nat Genet* **43**, 547-553.

Okano-Uchida, T., Okumura, E., Iwashita, M., Yoshida, H., Tachibana, K. and Kishimoto, T. (2003). Distinct regulators for Plk1 activation in starfish meiotic and early embryonic cycles. *Embo J* **22**, 5633-5642.

Pathi, S., Pagan-Westphal, S., Baker, D. P., Garber, E. A., Rayhorn, P., Bumcrot, D., Tabin, C. J., Blake Pepinsky, R. and Williams, K. P. (2001). Comparative biological responses to human Sonic, Indian, and Desert hedgehog. *Mech Dev* **106**, 107-117.

Rogers, K. W. and Schier, A. F. (2011). Morphogen gradients: from generation to interpretation. *Annu Rev Cell Dev Biol* **27**, 377-407.

Rohatgi, R., Milenkovic, L. and Scott, M. P. (2007). Patched1 regulates hedgehog signaling at the primary cilium. *Science* **317**, 372-376.

Shimada, A. and Takeda, H. (2008). Production of a maternal-zygotic medaka mutant using hybrid sterility. *Dev Growth Differ* **50**, 421-426.

Spemann, H. and Mangold, H. (2001). Induction of embryonic primordia by implantation of organizers from a different species. 1923. *Int J Dev Biol* **45**, 13-38.

Tanaka, M., Kinoshita, M., Kobayashi, D. and Nagahama, Y. (2001). Establishment of medaka (Oryzias latipes) transgenic lines with the expression of green fluorescent protein fluorescence exclusively in germ cells: a useful model to monitor germ cells in a live vertebrate. *Proc Natl Acad Sci U S A* **98**, 2544-2549.

Turing, A. M. (1952). The Chemical Basis of Morphogenesis.

Wheatley, D. N. (1995). Primary cilia in normal and pathological tissues. *Pathobiology* **63**, 222-238.

Wilson, C. W. and Chuang, P. T. (2010). Mechanism and evolution of cytosolic Hedgehog signal transduction. *Development* **137**, 2079-2094.

Wilson, C. W., Nguyen, C. T., Chen, M. H., Yang, J. H., Gacayan, R., Huang, J., Chen, J. N. and Chuang, P. T. (2009). Fused has evolved divergent roles in vertebrate Hedgehog signalling and motile ciliogenesis. *Nature* **459**, 98-102.

Wolff, C., Roy, S. and Ingham, P. W. (2003). Multiple muscle cell identities induced by distinct levels and timing of hedgehog activity in the zebrafish embryo. *Curr Biol* **13**, 1169-1181.

Xia, L., Jia, S., Huang, S., Wang, H., Zhu, Y., Mu, Y., Kan, L., Zheng, W., Wu, D., Li, X., et al. (2010). The Fused/Smurf complex controls the fate of Drosophila germline stem cells by generating a gradient BMP response. *Cell* **143**, 978-990.

Xiong, F., Tentner, A. R., Huang, P., Gelas, A., Mosaliganti, K. R., Souhait, L., Rannou, N., Swinburne, I. A., Obholzer, N. D., Cowgill, P. D., et al. (2013). Specified neural progenitors sort to form sharp domains after noisy Shh signaling. *Cell* **153**, 550-561.

Yamamoto, T. (1956). The physiology of fertilization in the medaka (Oryzias latipes). *Exp Cell Res* **10**, 387-393.

Yasumasu, S., Iuchi, I. and Yamagami, K. (1989). Purification and partial characterization of high choriolytic enzyme (HCE), a component of the hatching enzyme of the teleost, Oryzias latipes. *J Biochem* **105**, 204-211.

Yokoi, H., Shimada, A., Carl, M., Takashima, S., Kobayashi, D., Narita, T., Jindo, T., Kimura, T., Kitagawa, T., Kage, T., et al. (2007). Mutant analyses reveal different functions of fgfr1 in medaka and zebrafish despite conserved ligand-receptor relationships. *Dev Biol* **304**, 326-337.

Zimmermann, K. W. (1898). *Beiträge zur Kenntnis einiger Drüsen und Epithelien*.

Acknowledgements

I am using this opportunity to express my gratitude to everyone who supported me throughout the course of my research.

First and foremost, I would like to express my deepest appreciation to my supervisor, Dr. Hiroyuki Takeda for his substantial support, encouragement and patience.

My sincere gratitude is reserved for the other members of my committee, Drs. Yoshitaka Oka, Masanori Taira, Manabu Yoshida and Mariko Kondo for their constructive advices and valuable comments to my doctoral thesis.

I would also like to express my special appreciation and thanks to Dr. Haruo Hagiwara for his experimental support on SEM analysis; to Dr. Keiichiro Kamura, Dr. Tadashi Ishiguro and Mr. Yohei Masuda for their contributions to the identification of *aA90* responsible gene and their help in starting this work; to Drs. Sumito Koshida, Tatsuya Tsukahara, Atsuko Shimada and other members of Takeda Laboratory for their helpful discussions and suggestions; to Ms. Yasuko Ozawa for her excellent fish care.

Finally, I am greatly indebted to my family, Kayoko, Uichiro and Fumiko Yamamoto. Words cannot express how grateful I am for their heartfelt support, encouragement, suggestions and unconditional affection without which I would not have accomplished this study.